ChemComm

Accepted Manuscript

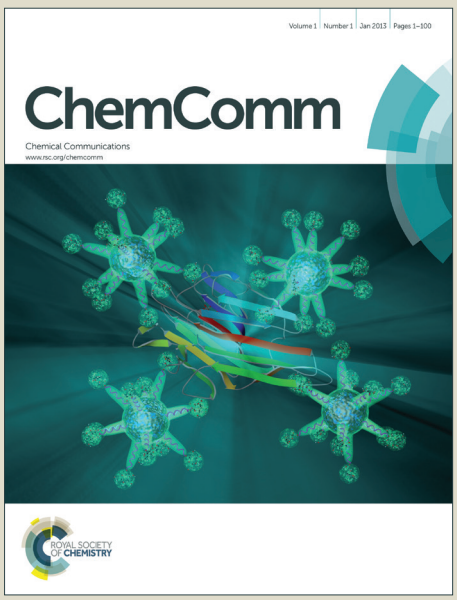

ROYAL SOCIETY OF CHEMISTRY

www.rsc.org/chemcomm

Journal Name

RSCPublishing

ARTICLE

Nitroarene reduction: A trusted model reaction to test nanoparticle catalyst

Cite this: DOI: 10.1039/x0xx00000x

Teresa Aditya,[a] Anjali Pal[b] and Tarasankar Pal*[a]

Received ooth January 2012,
Accepted ooth January 2012

DOI: 10.1039/x0xx00000x

www.rsc.org/

ABSTRACT:
Nitrophenol reduction to aminophenol with a reducing agent is conveniently carried out in aqueous medium mainly with a metal or metal oxide catalyst. This reduction is presently considered as a benchmark reaction to test a catalyst nanoparticle. Thousands of original reports have enriched this field of nanoparticle catalyzed reaction. Synthesis of different metal and metal oxide nanoparticles and their composites along with their role as catalyst for nitrophenol reduction with varying reducing agents have been elucidated here. The progress of the reaction is conveniently monitored by UV-Visible spectrophotometry and hence it becomes a universally accepted model reaction. In this review we have discussed the reaction kinetics considering its elegance and importance enlightening the long known Langmuir-Hinshelwood mechanism and Eley-Rideal mechanism at length, along with a few other mechanisms recently reported. A brief description of the synthetic procedures of various nanoparticles and their respective catalytic behaviour towards nitroarene reduction has also been accounted here.

Introduction

Metallic nanoparticle (MNp) has already left their promise in different fields of scientific and technological research. Now the world of catalysis involving MNp has been revolutionized and awaiting a sea change. In this regard semiconductor supported gold nanoparticle (AuNp) for activation of dioxygen deserve special mention. Supported[1,2] gold catalyst plays significant role especially for gas phase reaction. However, for liquid phase catalyzed reaction catalytic property seems to depend less on the support on which the catalyst rests. It has now been proved beyond doubt that catalysis involving MNp depends not only on the size but also on the shape and surface of the catalyst particle as well. Of late, facet[3] selective catalysis has elaborated finer details in catalysis. Naked particles are useful mostly for homogeneous catalysis and supported catalyst for heterogeneous ones. Active support for a catalyst for nitrophenol reduction has not been tried. However thought provoking usage of surface area, porosity, facet selection and heterojunction, etc. has been found to change the potential of a catalyst dramatically. The shift of Fermi level for MNps relate to their size dependent redox property. The size and shape selective catalysis in liquid phase is demonstrated taking supported and unsupported catalysts which are evidenced by the modern characterization techniques. Various types of metals[4], metal oxide[5] and bimetals[6] in their various compositions are widely explored for the catalysis of nitrophenol reduction in this review.

Nitrophenol and its derivatives are significant by-products produced from pesticides, herbicides and synthetic dyes.[7-9] 4-Nitrophenol (4-Nip) is well known to cause damage to the central nervous system, liver, kidney and both animal and human blood. Hence its removal from the environment is a crucial task. The reduction of 4-Nip is also essential in pharmaceutical industries for the manufacture of analgesic, antipyretic and other drugs, in photographic developer, corrosion inhibitor, anticorrosion lubricant, etc.[10-12]

To study the efficacy of any MNp in a catalytic process it is important to find a model reaction. The reaction must be convincing, trustworthy and should have a universal appeal so that the reaction can be studied with certainty using a simple

experimental set up. Till today only one reaction stands on a strong footing and has been qualified to study MNp catalyzed reaction that is an aqueous phase reduction reaction of 4-nitrophenol (4-Nip) to 4-aminophenol (4-Amp), and has been tested in different laboratories. The reduction reaction is a straight six electron transfer process in the presence of a reductant, sodium borohydride ($NaBH_4$). Any common MNp can be employed as a catalyst for this reaction. This reduction is ideally considered to proceed through a number of stages. But under the ambient experimental conditions it has been observed to pass through two distinct isobestic points. Thus it is corroborating a straight forward process to produce only 4-aminophenol without any side product. This reaction has been widely exploited for the study of catalytic activities thus confirming the synthesis of efficient nanoparticle catalyst[13-33] and can be entrusted as a model reaction. Additionally, it not only ensures the hasty depletion of hazardous nitrophenol from the environment using meagre amount of catalyst, but also proves to be beneficial. The reaction if selectively carried out yields functionalised aniline which becomes industrially useful in pharmaceuticals, polymers, herbicides and other chemicals.[34,35]

NMR Characterisation of the Reaction Product and Spectral Monitoring:

The unique reaction is conveniently carried out in simple laboratory set up using UV-light source. The product yielded after the reduction of 4-nitrophenol in presence of $NaBH_4$ and metal nanaoparticle catalyst has been attested to be 4aminophenol by NMR spectroscopy, as given below.

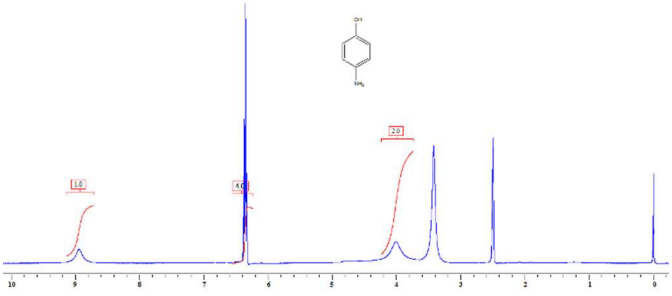

Fig. 1 ^1H NMR spectra of 4-aminophenol (300 MHz, d_6-DMSO, ppm)

From the NMR data reported, the OH group appeared at δ 9 ppm, NH_2 appeared at δ 4 ppm and the 4 aromatic H's appeared at δ 6.4 ppm, thus confirming the sole product to be aminophenol. The product of this reaction for various nitroarene compounds have been investigated with NMR studies which authenticate the products to be their corresponding amines.[36-41]

The substrate 4-Nip is yellow in water and that aids to study the kinetics of the reaction spectrophotometrically. Furthermore, the nitrophenolate ion at higher alkaline pH (pH > 12.0) increases the spectrophotometric sensitivity of the method that can be followed using a simple visible spectrophotometer only. The uncatalyzed reaction does not proceed favourably well in the forward direction and hence MNp plays its role to catalyze the reduction process. It has been spelt out that both the reactant and the reductant get adsorbed onto the MNp surface for the electron transfer to occur. Thus the absorbance of the reactant (λ_{max} = 400 nm) decreases noticeably with time. Concomitantly the absorbance of the product 4-Amp at its λ_{max} 296 nm increases. One can follow the 1st order reaction rate at a high concentration of borohydride (BH_4^-) taking a quantitative measure of any one of the two absorbance profiles i.e., the reactant or the product respectively. A temperature dependent study reveals the activation energy ~ 44 kJ mol^{-1} for such a reaction.

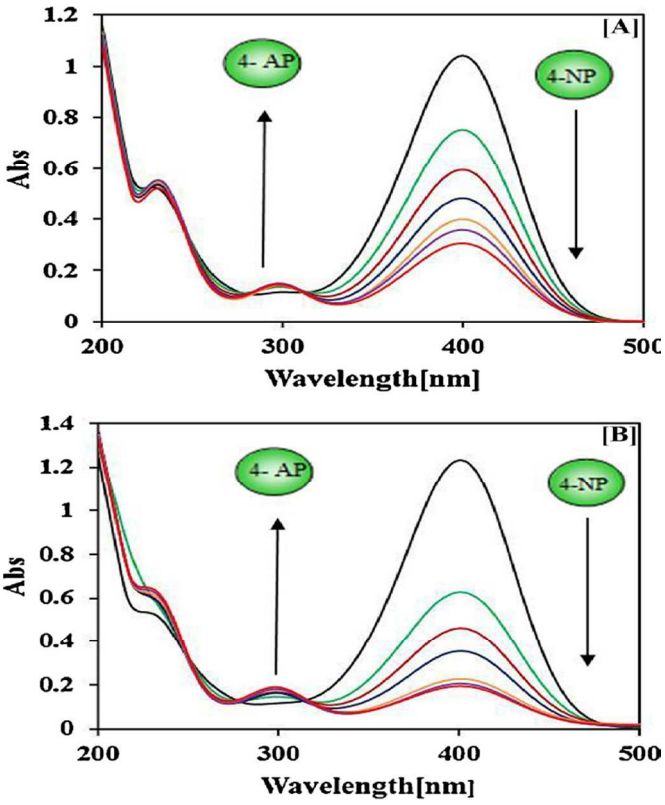

Fig. 2 UV–visible absorption spectra for the reduction of 4-nitrophenol to 4-aminophenol measured at 10 min time interval [A] at 25◦C [B] at 35◦C.

In aqueous solution highly diffusing borohydride ion and nitrophenolate ion both get adsorbed onto the catalyst surface. Then the electron transfer takes place which follows Langmuir-Hinshelwood mechanism (discussed later). The product, 4-Amp devoid of any chromophore imparts no colour to the aqueous solution and hence does not hamper the spectrophotometric determination.

Thermodynamically the reduction of 4-Nip to 4-Amp (E^o = -0.76V) at ambient condition is favourable as borohydride in water is a strong reductant (E^o = -1.33V). The reduction reaction in absence of MNp does not proceed in the forward

direction under the experimental time scale because of the kinetic barrier. The barrier is judiciously by-passed through the deployment of any common MNp catalyst and even catalysts with a huge support. In the reduction process the electron relay takes place irreversibly. Recently the mechanistic implication of the Eley-Rideal (discussed later) model has been discussed which suggest hydrogen adsorption on the catalyst surface for the reduction to occur. Exactly how MNps flank the surface atoms to accommodate 4-Nip and 4-Amp molecules remain unclear.

In this era of science metal nanoparticle has been a subject of immense interest because of their catalytic activity.[42-48] Particularly, redox reactions are efficiently catalyzed by nanoparticles as studied by many workers.[49-53] The quantification of the catalytic property was made possible by nitrophenol reduction which yielded aminophenol without any by-products.[54] The progress of the reaction can be conveniently measured by UV-Visible spectroscopy leading to the rate constant[55] and isobestic points to prove the absence of side reactions.[56]

The nitrophenol reduction can also be monitored by surface enhanced Raman scattering (SERS) spectroscopy that has been exploited by a number of scientists. Based on density functional theory (DFT) calculations SERS spectra can be simulated rendering improved theoretical approach. With the help of this method differences in Raman band enhancement factors can be determined. Ozaki *et al*.[57] used 4-nitrophenol to measure its SERS spectrum in a Ag colloidal solution and simulated with the DFT calculations. The DFT studies showed that the adsorption of 4-Nip was due to Coulombic interactions. According to the works of Sukhishvili *et al*.[58] oxidation of the Ag nanoparticle surface dramatically influence the adsorption, orientation, and SERS detection of nitroaromatic molecules in aqueous solution. In absence of oxidation of the surface-immobilized Ag particles, ultra-sensitive SERS detection of p-nitrophenol can be achieved. The silver oxide particles formed on the surface of the nanoparticle hinders charge transfer between the aromatic ring of the nitrophenol and the Ag metal which results in a decreased sensitivity of detection.

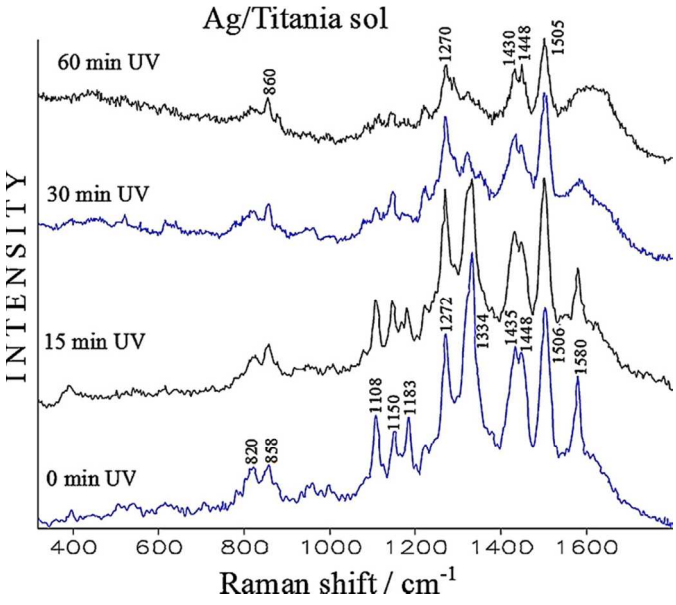

Fig. 3 The SERS spectra of 4-nitrophenol at different time intervals after treating with Ag/titania nanoparticle.

According to the works of Muiniz-Miranda[59] the nitrophenol adsorbs on the Ag doped surface. The strongest SERS band is observed at 1330 cm^{-1} due to the symmetric stretching mode of nitro group and there are also weaker bands below 1100 cm^{-1}. A downshift of SERS band to 1334 cm^{-1} from Raman band at 1342cm^{-1} implies a chemical interaction of the substrate through the nitro group which is at par with the DFT calculations for 4-Nip.[57] SERS bands around 1440cm^{-1}, 1500cm^{-1} and 1580 cm^{-1} are considered to be the vibrational modes of the molecules. On further being exposed to UV irradiation the intensity in the nitro group SERS band decreases till it disappears along with other bands. Such a disappearance is attributed to the lack of interaction of the aminophenol with the Ag/titania nanoparticle. The Ag/titania nanoparticles show catalytic activity by supplying electron for the following reaction,

$$R\text{-}NO_2 + 4H+ + 6e^- \longrightarrow R\text{-}NH_2 + 2OH^-$$

Thus spectral study conveniently monitors the progress of the reaction and it is a well-established protocol to testify the catalytic activity of the as-synthesised metal nanoparticles.

Reaction Medium

The reaction medium is mostly basic as sodium borohydride in aqueous medium splits to give borohydride anion and sodium cation which makes the solution basic in nature. In most of the cases this is the situation but in few cases the reduction in an acidic medium has been reported as well, like in the works of Ding et al.[60] They prepared a nanocomposite in absence of any noble metal and used it for the catalysis of hydrogenation reaction in acidic medium.

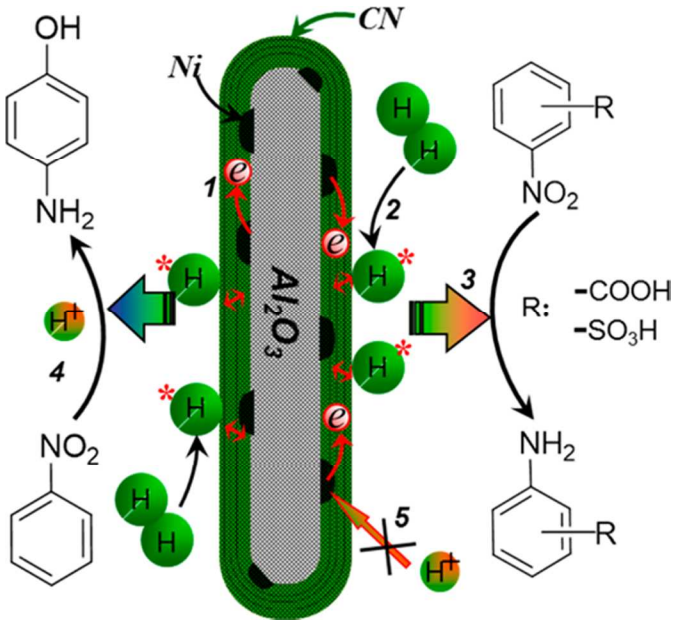

Fig. 4 Schematic representation of the principle of mesostructural CN catalyst with nickel lying under it. The points are as follows (1) donation of electron from nickel to CN, (2) dissociative adsorption of the hydrogen molecule which bonded to the CN surface, (3) the nitro compound reduced by the activated hydrogen, (4) under strong acidic condition the adsorbed hydrogen is capable of hydrogenation, where concentrated protons take part in the reaction for the rearrangement of the intermediate and (5) the protection of nickel from corrosion or poisoning.

Nanocomposite involving carbon nitride (CN) with nickel has been prepared where the latter bestows on the CN moiety new active sites for adsorption of hydrogen and activation, which otherwise remain inactive during hydrogenation. However, Ni itself remain inert to the reaction and is barred from poisoning or loss. Nitrobenzene reduction has been performed in acidic medium involving H_2SO_4. Metallic Ni in the composite remain as a cationic site donating its electrons to the adjacent CN thereby rendering accessible hydrogen adsorption sites. Thus establishing a symbiotic nanocomposite where Ni is protected from the corrosive action of acid by inert CN whereas the CN is endowed with hydrogen adsorption and activation ability by Ni. There are a handful of references for the preparation of metal nanoparticles in organic solvents.[61-67] However, nitrophenol reduction in most cases proceeds via nitrophenolate ion which is prompted in aqueous medium. Hence this maybe the main reason that investigators mostly have not accounted nitroarene reduction in organic medium.

Kinetics of the Reduction Reaction

Ballauff *et al.*[68] in their study of nitrophenol reduction with $NaBH_4$ explained the reaction kinetics of the reduction. In the direct route nitrobenzene is reduced to nitrosobenzene and consecutively to phenyl hydroxyl amine which is the first stable intermediate, finally leading to the formation of aniline. Hence, taking nitrophenol substrate it can be schematically written as 4-Nip → 4-nitrosophenol → 4-hydroxylaminophenol → 4-Amp as illustrated by Siadatnasab.[69]

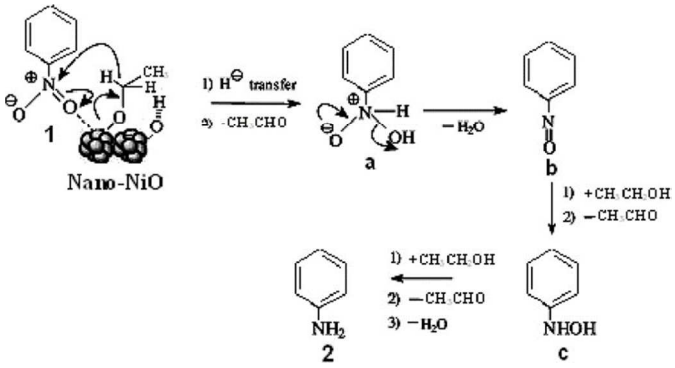

Fig. 5 The various intermediates of nitrophenol reduction with NiO nanoparticle catalyst prepared via thermal decomposition of the bis(dimethylglyoximato)nickel(II) complex which is a novel reusable heterogeneous catalyst for fast and efficient microwave-assisted reduction of nitroarenes.

At the start of the reaction there is an induction time which is attributed to the rearrangement of the surface atoms of the nanoparticle before the progress of the reaction.

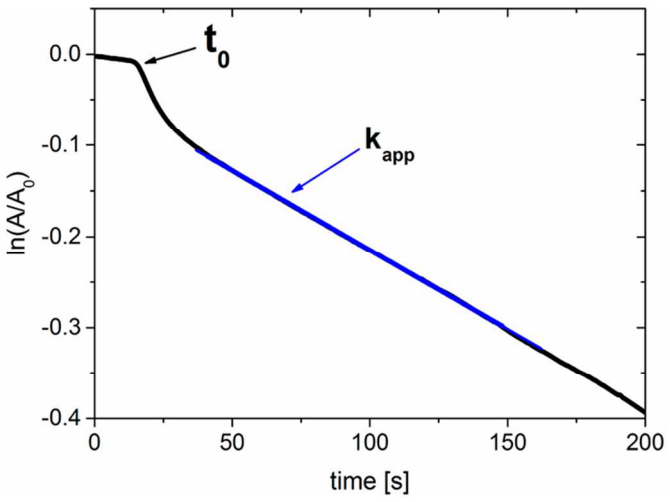

Fig. 6 A plot of typical time dependence of the adsorption of 4-Nitrophenolate ions at 400 nm. The blue coloured part of the line displays the linear section from which K_{app} is taken and the black arrow indicates the induction period t_0.

Hence, the compounds that compete to undergo adsorption and desorption cycle with the fixed number of sites of the metal surface are 4-Nip , 4-hydroxylaminophenol (Hx) and 4-Amp, the concentrations of which are written as C_{Nip}, C_{Hx} and C_{Amp}, respectively. The surface coverage by 4-Nip, 4-hydroxylaminophenol and BH_4^- being θ_{Nip}, θ_{Hx} and θ_{BH4} respectively and taking K_{Nip}, K_{Hx} and K_{BH4} as the Langmuir

adsorption constant of the respective compounds. From Langmuir-Freundlich isotherm we have

i. $$\theta_{Nip} = \frac{(K_{Nip}C_{Nip})^n}{1+(K_{Nip}C_{Nip})^n + K_{Hx}C_{Hx} + K_{BH4}C_{BH4}}$$

Where, n is the Langmuir-Freundlich exponent which is set at 0.5 for Nip and to 1 for Hx and BH_4^-. This way θ_{Hx} and θ_{BH4} can also be formulated.

Hence, the rate of the reduction of Nip with BH_4^- was denoted by

ii. $$-\frac{dC_{Nip}}{dt} = K_{app}C_{Nip} = K_aS\theta_{Nip}\theta_{BH4} = \left(\frac{dC_{Hx}}{dt}\right)_{source}$$

Where, K_{app} is the decay rate constant and S is the total surface area of all the catalyst nanoparticle in solution. $S\theta_{Nip}$ is proportional to the number of adsorbed substrate molecules in the system and θ_{BH4} denotes probability to find a hydrogen ion adsorbed in the vicinity of Nip. There is no detectable change in concentration of the solution due to equilibrated and small adsorption of the substrate on the catalyst surface. The reduction can be assumed to be taking place in two steps

4-Nip → 4-hydroxylaminophenol → 4-Amp

The rate of reduction of Nip to Hx is as follows

iii. $$-\frac{dC_{Nip}}{dt} = K_aS\frac{(K_{Nip}C_{Nip})^nK_{BH4}C_{BH4}}{\left\{1+(K_{Nip}C_{Nip})^n + K_{Hx}C_{Hx} + K_{BH4}C_{BH4}\right\}^2} = \left(\frac{dC_{Hx}}{dt}\right)_{source}$$

Where, K_a is the rate constant for this conversion.

The rate of conversion of intermediate Hx to Amp is as follows

iv. $$-\left(\frac{dC_{Hx}}{dt}\right)_{decay} = K_bS\frac{(K_{Hx}C_{Hx})^nK_{BH4}C_{BH4}}{\left\{1+(K_{Nip}C_{Nip})^n + K_{Hx}C_{Hx} + K_{BH4}C_{BH4}\right\}^2} = \frac{dC_{Amp}}{dt}$$

Where, K_b is the rate constant for this conversion.

Hence, the rate equation for the intermediate Hx is as follows

v. $$\frac{dC_{Hx}}{dt} = \left(\frac{dC_{Hx}}{dt}\right)_{source} - \left(\frac{dC_{Hx}}{dt}\right)_{decay}$$

Now, $K_a >> K_b$ as we see from the first order kinetics of this reaction that formation of Hx occurs at a greater rate than its depletion hence there is a decrease in concentration of the Nip and a steady state of Hx is obtained, consequently a small production of aminophenol is observed. A competition occurs with Nip when the concentration of Hx rises in the solution as the affinity of the latter to the catalyst surface is more. However, we can neglect the adsorption of the Amp as it has no effect on the rate. After the initial state there is a stationary state which can be written as

vi. $$\frac{dC_{Hx}}{dt} = 0$$

The reaction above can be written in two forms

- Early time period from t_0 to t_s, when $C_{Hx} \approx 0$ and follows the equation (i), where t_0 is the time before the reaction starts and t_s is the beginning of the stationary state.
- Stationary state ($t > t_s$), when C_{Hx} is approximately constant and can be written as

vii. $$C_{Hx,stat} = \frac{K_a(K_{Nip}C_{Nip})^n}{K_bK_{Hx}}$$

Therefore, we get from (iii)

viii. $$-\frac{dC_{Nip}}{dt} = K_aS\frac{(K_{Nip}C_{Nip})^nK_{BH4}C_{BH4}}{\left\{1+(K_{Nip}C_{Nip})^n\left(1+\frac{K_a}{K_b}\right)+K_{BH4}C_{BH4}\right\}^2} = \frac{dC_{Amp}}{dt}$$

At this stage the formation of aminophenol is equal to the depletion of nitrophenol, the concentration at this stage must be small for isobestic point to arise. We get tangent of absorbance as the function of time in the two limiting times of -

- From t_0 to t_s

ix. $$K_{app,I} = K_aS\frac{(K_{Nip}C_{Nip})^{n-1}K_{BH4}C_{BH4}}{\left\{1+(K_{Nip}C_{Nip})^n + K_{BH4}C_{BH4}\right\}^2}$$

- For t >ts

x. $$K_{app,II} = K_aS\frac{(K_{Nip}C_{Nip})^{n-1}K_{BH4}C_{BH4}}{\left\{1+(K_{Nip}C_{Nip})^n\left(1+\frac{K_a}{K_b}\right)+K_{BH4}C_{BH4}\right\}^2}$$

Hence, we can conclude that the $C_{Hx,stat}$ at $t = t_s$ must be the total concentration of nitrophenol decayed by that time. For t=0 the concentration of nitrophenol is $C_{Nip,0}$. Therefore for time t we can write

xi. $$\ln\frac{C_{Nip,0} - C_{Hx,stat}}{C_{Nip,0}} = -K_{app,I}(t_s - t_0)$$

xii. $$(t_s - t_0) = \frac{C_{Hx,stat}}{C_{Nip,0}K_{app,I}} = \frac{\{1+(K_{Nip}C_{Nip,0})^n + K_{BH4}C_{BH4}\}^2}{K_bSK_{BH4}C_{BH4}K_{Hx}}$$

xiii. $$K_{app,II} = K_aS\frac{(K_{Nip}C_{Nip})^{n-1}K_{BH4}C_{BH4}}{\left\{1+(K_{Nip}C_{Nip})^n + K_{BH4}C_{BH4}\right\}^2}$$

Hence, taking into account all the factors of stationary state when $K_a << K_b$, equation xiii is appropriate and the reduction of 4-Nip is the rate determining step. Whereas, when $K_a >> K_b$ reduction of 4-hydroxylaminophenol is the rate determining step.

In the presence of excess $NaBH_4$ and adequate amount of catalyst the reaction is a pseudo first order reaction and is mostly dependent on the concentration of 4-Nip, which gets adsorbed on the surface of the catalyst with its two oxygen atoms. Hence the initial adsorption of the 4-nitrophenol to the catalyst surface is associated to the rate constant for the full reaction. The influence of electronic structures of metals particularly the d-band centre on catalytic activity was propounded by Newns[70] and detailed by Hammer and Norskov[71] for nitroarene reduction.[72] Bronsted-Evans-Polanyi (BEP) relation explains that rate of first order surface reaction is higher in cases where there is strong adsorption energy to the surface. In BEP relations strong binding regime shows smallest activation energy whereas in weak binding regime the activation energy is high. The efficient catalysts attain an optimal condition in which the energy barrier is low enough to be overcome and such that the adsorbed molecules can later diffuse and desorb from its surface. As soon as the d-band of the metal and the adsorbate, nitrophenol in this case, interact the states of both combine and further split into a bonding and an antibonding level. The d-band goes further below the Fermi level and the antibonding state gradually gets more populated resulting into a weakening of the chemisorption strength. Net

repulsion results from bonding and antibonding population which increase with an increase in size of the specific metal. Exploiting this idea bimetallic nanocatalysts are brought into picture. The bimetals to be tuned are chosen such that one of them are inactive due to strongly bonded reactants along with another that is inactive due to weakly bonded reactants. The balance between these regimes have been exploited in the volcano plot.[73] A very strong binding of the adsorbate and catalyst will prevent any further reaction to occur whereas a very weak binding will not cause the adsorbate to interact with the catalyst. The peak in the volcano plot occurs in places where these two effects are balanced. The centre of the d-band of the metal surface is the primary factor for controlling the chemisorption strength. With the help of this scatter plot of turnover frequency as a function of adsorption energy and by tuning dendrimer composition in bimetallic dendrimers[74-76] Stevenson and Henkelman[77] designed catalyst for nitrophenol reduction with the adsorption energy closest to the peak avoiding the weak and strong binding limits in the plot.

The Reduction Mechanism

Nitrophenol reduction to aminophenol takes place in the presence of reducing agent and a catalyst. There exists a number reported mechanisms.

➢ **Langmuir – Hinshelwood Mechanism (LH) :**

This mechanism of reduction involves the surface adsorption of the reducing agent and the nitrophenol substrate on the catalyst.[78-80] There is a possibility of intermediate as well.[81,82] The hydrogen ion from the catalyst transfers in the substrate and reduces it. This mechanism has been discussed by Ballauff *et al.*[83] following the Langmuir adsorption isotherm.

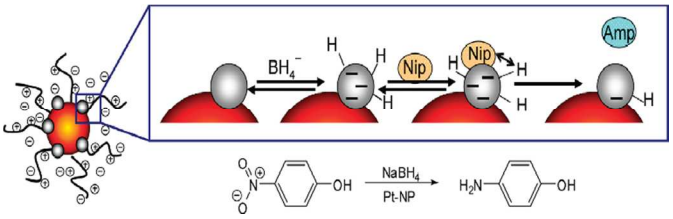

Fig. 7 A schematic representation of the LH mechanism.

The borohydride ion transfers hydrogen on the surface in a reversible manner and the nitrophenol is reduced. The rate-determining step consists of the reduction of nitrophenol by the surface hydrogen species. The reaction rate can therefore be related to the total surface S of the nanoparticles, the kinetic constant K related to the rate-determining step, and the adsorption constants K_{Nip} and K_{BH4} of nitrophenol and borohydride, respectively. In all the cases, of the order of minutes an induction time t_0 was observed. The reciprocal induction time can be treated as a reaction rate that is directly related to the kinetics of the surface reaction because there is a linear relation between $1/(Kt_0)$ and the concentration of nitrophenol in the solution. All data obtained for t_0 so far and a comparison of these data from literature indicates that the induction time is related to a slow surface reconstruction of the nanoparticles, the rate of which is directly related to the surface reaction.

➢ **Eley – Rideal Mechanism (ER) :**

This mechanism has also been used to explain the reduction process.[84-87] Surface molecule electron transfer processes in hyperthermal surface ionisation of organic molecules has been widely studied.[88-91] Study on dissociative ionisation[92-95] and its relation to collision induced dissociation has been carried out. The mechanism does not lay emphasis on substrate or reducing agent adsorption on the catalyst. Rather it states that hydrogen atom remains adsorbed on the surface of the catalyst which is captured by the substrate i.e. nitrophenol upon collision. Potential-energy barrier for further interactions, like chemisorption, reaction, dissociation, and ionization has been studied.[96-98] The threshold energy for the abstraction of the adsorbed hydrogen atom from the surface of the catalyst must be equal to the difference of the surface work function of the catalyst and the ionisation potential of the substrate.[99] Hence, high energy incident light can cause ionization as this potential barrier is overcome.[100]

The LH and ER mechanism can be differentiated by the dependence of reaction rate on pressure of the reagents.

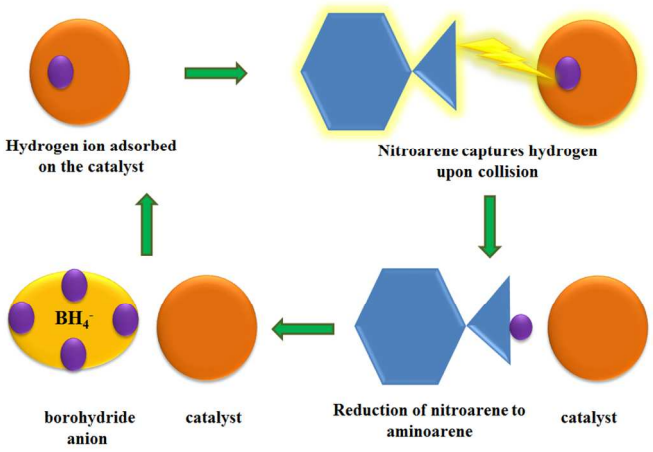

Fig. 8 A schematic representation of the ER mechanism.

➢ **Semiconductor Mechanism :**

This mechanism was proposed by Pradhan *et al.*[101] where capped metal (sol) semiconductor was used to reduce nitrophenol under UV-light in the presence of $NaBH_4$. When UV-light is used on the metal semiconductor an exciton is produced under its band edge excitation. An electron from the valence band is transferred to the conduction band creating a hole and a free electron. This free electron can reduce organic molecule like the nitrophenol reduction to aminophenol. The sodium borohydride supplies electron being a sacrificial donor. Again, when ZnS is doped with Mn or Cu this reduction is

either stopped or proceeds at slow rate, respectively. The reason is that the electron[102] from the conduction band of Zn in the first case successfully reduces the nitrophenol by reaching its LUMO, whereas in the next two cases the electron gets recombined by the $^4T_1$-$^6A_1$ states of the Mn and Cu, which is relatively slow in the third case due to larger difference in band gap energy.

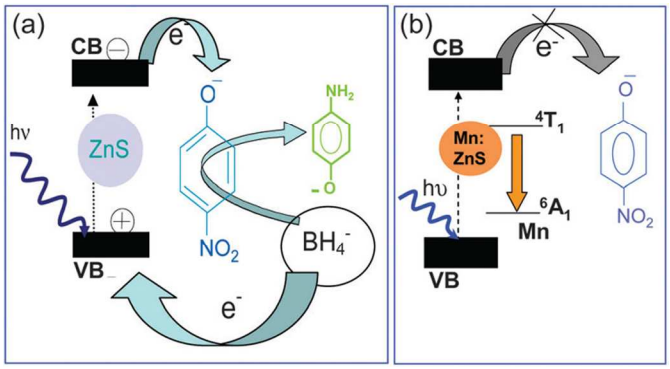

Fig. 9 A schematic representation of the semiconductor mechanism.

➢ **Defect-mediated mechanism :**

Apart from this Wang *et al.*[103] synthesised noble-metal-free highly reactive and recyclable TaO_xN_y from the nitridation of $Ta_{1.1}O_{1.05.}$ They utilised this nanocatalyst to reduce nitrophenol and suggested a new mechanism. From previously reported papers it is known that in N-doped TiO_2 nitrate and imino functionality coexist. The imino group is the incomplete oxidation of the nitrate which can be oxidized completely to produce nitrate.[104] In nanocrystal of TaOxNy the nitrate species bind with hydride ions of BH_4^- and transform to metastable iminoborohydride. The oxygen vacancies which can act as the active sites for the capture of oxygen of the nitric oxide[105] are instrumental in capturing the oxygen of the nitro group of 4-Nip. By the surface vacancy diffusion mechanism[106] mobile oxygen vacancies diffuse towards the metastable iminoborohydride species and can capture hydride ions from the vicinal site. Similar to Langmuir Hinshelwood mechanism, after completion of electron transfer and reaction of surface hydrogen from iminoborohydride the 4-Amp species desorbs from the surface and the trapped oxygen atoms in the lattice sites of BH_4^- is also released resulting into borate ions.

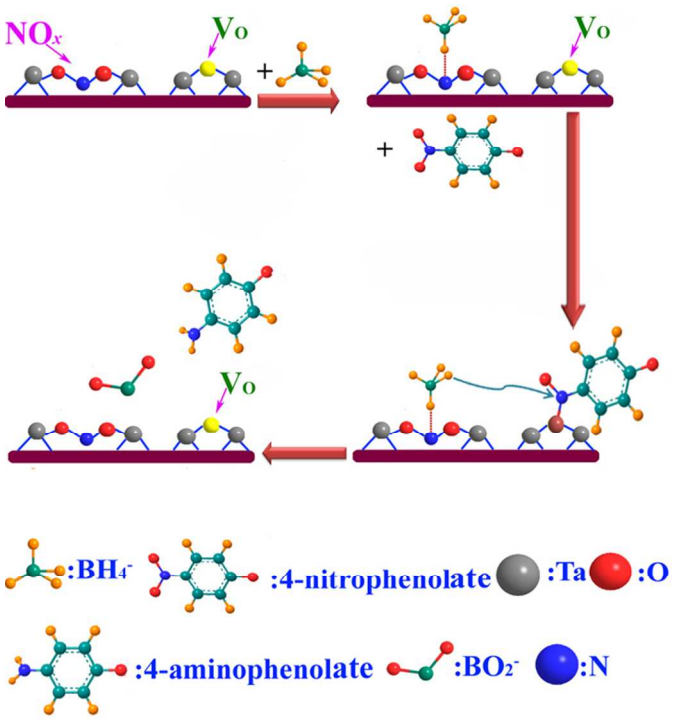

Fig. 10 A schematic representation of the defect-mediated mechanism and the probable reduction processes of 4-Nip on the surfaces of TaOxNy nanocrystals. Where V_0 represents the paramagnetic oxygen vacancies.

➢ **Photocatalytic mechanism :**

There are a number of papers reporting the reduction of nitrophenol with photocatalysts.[107] The concept of this reduction has been explained with respect to valence and conduction band in relation with the reduction potential of the catalyst, and the acceptor and donor components. The reduction potential of nitro compounds caused the selective reduction of nitro group in the presence of multifunctional groups of aromatic[102] and aliphatic nitro compounds. On irradiating the semiconductor catalyst with photons there develops positive holes in the valence band and negative electrons on the conduction band. These charge carriers can thereby participate in redox reactions. For example Havlinova *et al.*[108] in their work have discussed the formation of charge carriers in TiO_2[109,110] and their involvement in redox reactions.

$TiO_2 + h\nu \longrightarrow TiO_2 (e^- + h^+)$

The reduction potential of electrons of TiO_2 is E_{cb} = -0.80 V vs. SCE in acetonitrile. For electron acceptors with higher reduction potential ($E_{A/A^{-\cdot}}$) the negative charge carrier electrons of TiO_2 are readily available. This difference in energy between acceptor redox couple $E_{A/A^{-\cdot}}$ and TiO_2 E_{cb} is the driving force for the transfer of electrons.

$e^- + A \longrightarrow A^{-\cdot}$

The oxidation potential of holes in the valence band of TiO_2 is E_{vb} = 2.4 V vs. SCE in acetonitrile. For hole acceptors with lower oxidation potential ($E_{D/D^{+\cdot}}$) the positive charge carrier holes of TiO_2 are readily available.

$h^+ + D \longrightarrow D^{+\cdot}$

This difference in energy between acceptor redox couples and TiO_2 band gap level is the driving force for the transfer of electrons or holes.

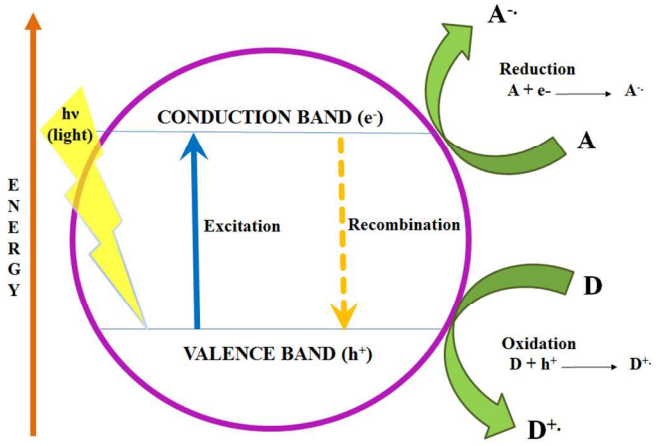

Fig. 11 A schematic representation of photocatalytic mechanism where excitation of electrons on the catalyst form electrons and holes (charge carriers).

When aliphatic alcohols are used as a solvent they get oxidised by photogenerated holes to produce carbonyl compounds by abstraction of α hydrogen w.r.t carbonyl carbon.

$R\text{-}CH_2\text{-}OH + h^+ \longrightarrow R\text{-}CH\text{-}OH + H^+$

$R\text{-}CH\text{-}OH \longrightarrow R\text{-}COH + {\cdot}H$

$2\ {\cdot}H \longrightarrow H_2$

Mahdevi *et al.*[102] proposed a mechanism which is affected by the electron transfer efficiency from the conduction band of TiO_2 to the nitro compound, the back electron transfer to the valence band from nitro radical anion and availability of proton.

Apart from the equations guiding the LH and ER mechanisms which were also applicable in this case, they additionally related the rate of 4-nitrophenol reduction by TiO_2 in the presence of alcohol with some solvent parameters:

1. Viscosity
   The viscosity, η, for the solvent significantly influenced the rate of nitrophenol reduction on TiO_2 and the linear dependence was given by the equation
   $\log K = -0.65 - 0.27\eta$ ($R^2 = 0.96$)
   The different values of K_{Nip} and K_{Amp} as evaluated from the exponential curves were tested to be used in one common data, R being the overall rate of the reduction reaction.
   Stokes-Einstein equation follows as
   $D = KT/6\pi r\eta$
   Where D is diffusion and r is the radius of the diffusing species.[111] Hence, the diffusion of the reaction intermediate to/from irradiated TiO_2 surface was influenced by the solvent viscosity. Since this reduction is complex the influence of solvent reorientation dynamics[112-114] on the reaction rate was not brought into consideration.
2. Solvent polarity[111]
   Y= (€s-1)/(€s+2)
   where €s is the relative solvent permittivity.
3. Solvent polarisability[111]
   $P = (n^2-1)/(n^2+2)$
   where n is the solvent refractive index for sodium D-line.
4. Solvent polarity/polarisability[115,116] parameter π^*, which measures the ability of the solvent to stabilise a charge or dipole with its dielectric constant.

Thus it could be concluded that these parameters together with the previously discussed reaction rate equations influence the reduction of 4-nitrophenol to 4-aminophenol in TiO2 photosensitised reaction in alcohol solvents.

A large number of scientists have studied the activation energy for the reduction by carrying out kinetic run at different temperatures.[117-119] Nitroarene reduction yielding aminoarene would supposedly follow similar mechanism.

Nanocatalysts

Noble Metal :

An enormous amount of work has been done with noble metals for the reduction of nitrophenol.

We have carried out a large number of work out of which few have been mentioned. We have worked with coinage metals[54] (Au, Ag, Cu) and prepared full-grown microelectrode (FGME) or still growing micro electrode (GME) from their metal salts in air or N_2 atmosphere under ice cold condition in presence of $NaBH_4$, or N_2H_4, or CO, or sodium ascorbate as reducing agent. These electrodes were then used for reduction of nitrophenol considering the size effect of the catalyst,[120] FGME and GME, which was detected with kinetic study.

We have further prepared Ag[36] nanoparticles *in situ* which catalyzed the reduction of nitroarenes in presence of $NaBH_4$. The kinetics of the reaction was studied with GME and FGME and the rate of reaction followed the order 4-Nip > 2-Nip > 4-nitroaniline.

In our preparation of mesoporous leafy nanostructures of Au and Pd[121] we used dihydropyridine ester (DHPE) as the reducing agent at room temperature, at the liquid-liquid interface of dichloromethane-water. Here DHPE lies in the former and chloroauric acid or palladium chloride lies in the latter phase. The porous palladium leaves could reduce 4-Nip by hydrazine hydrate at room temperature unlike the high temperature methods reported in the succeeding section.

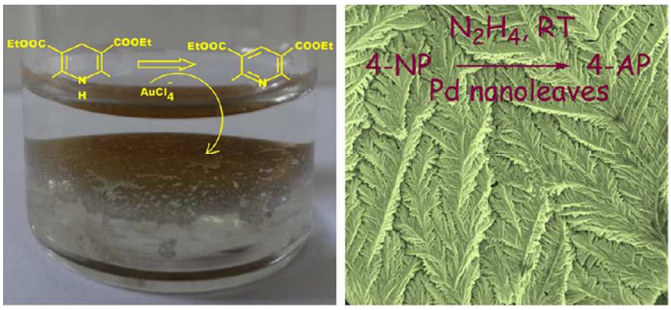

Fig. 12 Mesoporous nanocatalyst reducing 4-nitrophenol to 4-aminophenol in the presence of hydrazine at room temperature.

Preparation of bimetallic Pt-Ni nanoparticle[122] was conveniently carried out at room temperature with the help of a micellar solution containing the corresponding metal salts in a wet chemical method. Co-reduction of the respective salts produced alloys in bulk quantity, the composition of which could be varied with different ratios of the salt. Catalytic efficiency for nitrophenol reduction was studied and it was found to be greater for bimetallic Pt-Ni than monometallic Pt. The rate was dependent on the composition of the bimetallic Pt-Ni due to varying induction time.

We also prepared ferromagnetic ultra-long prickly nickel nanowires[123] in gram scale utilising a surfactant assisted mildly wet approach using $NiCl_4$ as precursor and hydrazine as the reducing agent. It was then used to catalyze 4-Nip reduction with $NaBH_4$.

Synthesis of silver nanoshell-coated polystyrene beads[124] by immobilization of silver precursor ion followed by wet chemical reduction at room temperature was carried out by us. Thereafter, it was used as a solid phase catalyst for nitrophenol reduction in the presence of $NaBH_4$. Immobilisation of precursor into resin beads was due to electrostatic field force. The rate of reduction of nitrophenol was found to be 4-Nip > 2-NiP > 3-NiP.

Patra and coworkers[125] has also worked on bimetallic core shells based on the Au/Ag core shell nanoparticles which he has utilised for nitrophenol reduction.

Astruc *et al.*[126] elucidated the effect of ligands on the catalytic efficiency in the nitrophenol reduction of Au[127] nanoparticles which are essentially electron reservoirs. The best stabilizer is concluded to be thiolate followed by citrate hence giving a low and high catalytic activity, respectively. The 1,2,3-triazole-stabilized Au Nps[128] are much more efficient in comparison to the former two.

Hou *et al.*[129] prepared platinum nanocatalyst mono-dispersed on reduced graphene oxide by simple reduction with ethylene glycol. This was more efficient than multi-walled carbon nanotubes (CNT) and active carbon as supports. The catalyst was dispersed in ethanol and substrate was added and purged with hydrogen at 1.0 MPa pressure at temperature 0-40°C.

In their work Kaur *et al.*[130] synthesised gold nanoparticles supported on resin Amberlite XAD-4 beads from gold chloride, ethanol and $NaBH_4$. The resin is neutral, non-functional, hydrophobic, macro-porous, commercial and cross-linked polystyrene. The nitrophenol reduction was carried out by adding the catalyst, methanol or water, nitro substrate and $NaBH_4$. In presence of halo group there is selective reduction of nitro group where as in presence of aldehyde or olefinic bond the latter gets preferentially reduced. On increasing the $NaBH_4$ concentration in the latter cases the nitro groups are further reduced.

Babaknezhad *et al.*[131] prepared Ni-NPs[132] as Ni-polyvinylamine/SBA-15 (Ni-PVAm/SBA-15) catalyst. Polyacryl amide, SBA-15 and benzoyl peroxide were heated at 70-75°C to make polyvinyl amine/SBA-15 (PVAm/SBA-15) composite. Next, $NiCl_2.6H_2O$ and water was heated at 80°C and methanol solution of $NaBH_4$ was added to give Ni-PVAm/SBA-15 composite. Then the nitro substrate was reduced by treating it with the prepared composite and $NaBH_4$. Increasing the amount of nanoparticle the reaction became more efficient.

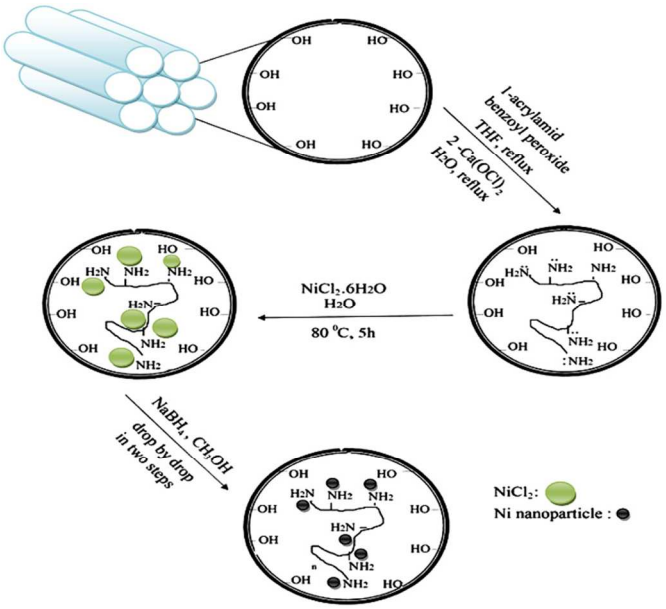

Fig. 13 Preparation of Ni nanoparticles-polyvinylamine/SBA-15 catalyst for the reduction of aromatic nitro compounds.

Li *et al.*[133] prepared selectively 5-fold twined nanowires and single twined right bipyramids of Pd in hydrophilic system. Difference in the strength of interaction between I^- and Cl^- would decrease the oxidative etching of O_2/halide pair differently thereby controlling the twined nanostructures of Pd. Nanowires have more twin boundaries hence it reduces 4-Nip faster than bipyramids.

Yada *et al.*[134] employed $H_2PtCl_6.6H_2O$ and gum acacia (GA) heated at 100°C and using acetone as anti-solvent the catalyst GA-Pt colloidal solution was prepared. Reduction of the nitro substrate was carried out with hydrogen balloon.

Huh *et al.*[135] prepared monodispersed Au/Au@polythiophene core or shell[136] nanospheres by reduction of $AuCl_4$- with 2-thiophenneactonitrile at room temperature in aqueous medium which in turn gets polymerised forming a conductive

polymer shell. With this Au/Au@polythiophene core/shell nanosphere both hydrophobic and hydrophilic nitroarenes were hydrogenated under mild conditions with $NaBH_4$ using nitrobenzene, nitrophenol and nitrotoluene as the substrates.

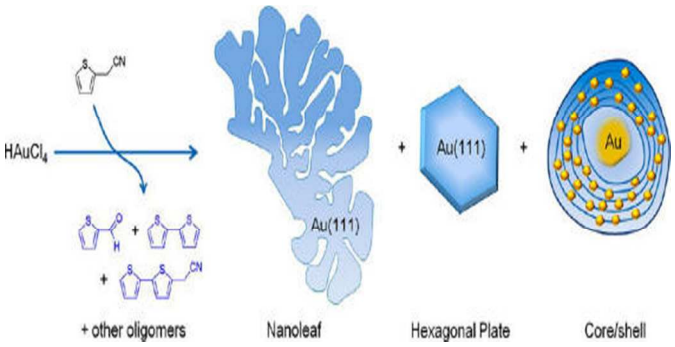

Fig. 14 Heterogeneous catalysis of nitroarenes with Au/Au@Polythiophene core/shell nanospheres.

Jiang and co-workers[137] prepared monodispersed silver nanocage (AgNC) containing well defined hollow interiors and well controlled size using NaCl as the template. The nanocatalyst was further used to catalyze nitrophenol reduction.

Huang *et al.*[138] prepared porous ionic copolymer with Rh nanocatalyst. The reduction was carried out by using nitrobenzene with hydrazine monohydrate as reducing agent at 60°C. The resulting catalyst efficiently reduced nitrophenol.

Li *et al.*[139] prepared bimetallic $Pd_1Ag_{1.7}$ controlling the composition of the investigational $Pd_{1-x}Ag_x$(x=0-1) which was generated by co-reduction of $Pd(acac)_2$ and $AgOOCCF_3$ using borane-tert-butylamine in oleylamine. Unlike Ag which is inactive, and Pd/C and Pd nanoparticles which have high activity but low selectivity, this bimetallic nanoparticle showed high selectivity but low activity. On increasing the ratio of Ag selectivity increased while reactivity decreased. The $Pd_1Ag_{1.7}$ nanocatalyst was found to be the best composition for optimal selectivity without loss of activity on taking benzaldehyde and nitro benzene

Fan *et al.*[140] deposited gold nanoparticles on TiO_2. They used this heterogeneous catalyst for reduction of nitroarenes directly with alcohols for 14 h at 120°C under Ar atmosphere. The alcohol here acts as the reducing agent for the nitroarene reduction. The dehydrogenation of alcohol gives carbonyl compound proceeding via gold-hydride species which then cause mono or di-N-alkylation.

Scott *et al.*[141] in their study using alkaline thiolate stabilizer prepared gold monolayer protected clusters[142,143] (Au-MPCs) in which gold thiolate bonds are reductively eliminated by strong reducing agent like sodium borohydride. This labile thiolate ligand can be utilised to control the growth of the Au-MPCs which in turn can be used as a catalyst to reduce small substrates such as 4-Nip.

Yang *et al.*[144] prepared rattle type or yolk-shell microsphere[145] consisting of a gold nanoparticle encapsulated[146] by amine group decorated SiO_2/poly(ethylene glycol dimethacrylate) rattle-type microsphere. The amine group acts as an anchor forming a siloxane linkage with the gold precursor, $AuCl_4^-$, which in turn gets reduced to Au nanoparticle by $NaBH_4$ and could be eventually used for 4-Nip reduction.

A similar kind of work has been conducted by Pinkhassik *et al.*[147] where he prepared metal growing inside hollow capsules.[148-151] Tannic acid(TA), *β*-cyclodextrin(*β*-CD)[152], and polyether dendrimer acts as the sacrificial molecules which are trapped inside the nanocapsule[153-158] and is instrumental in synthesising the metal nanoparticle. These initiators can be conveniently removed by the application of acid hydrolysis. The metal can then be utilised for nitrophenol reduction.

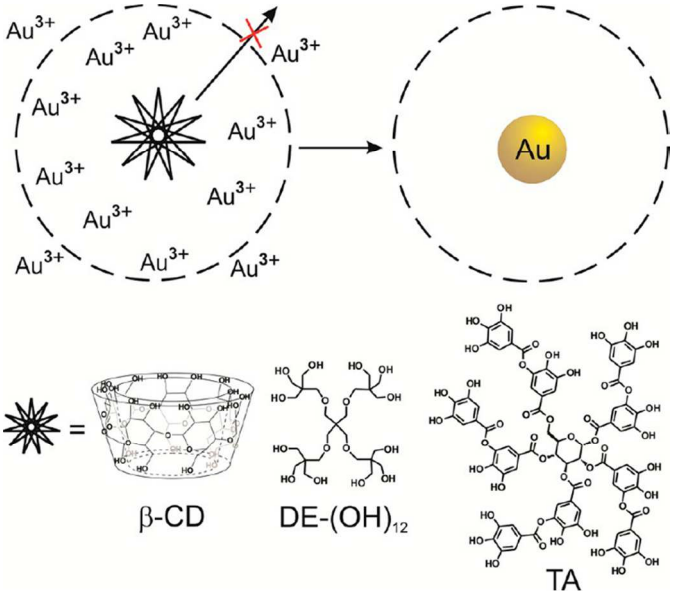

Fig. 15a An entrapped initiator is unable to escape from the capsules, but metal ions are able to enter the capsule freely. The initiators used in this case were β-cyclodextrin (β-CD), polyol dendrimer ($DE-(OH)_{12}$), and tannic acid (TA). After the synthesis, metal NPs remain permanently entrapped in the nanocapsules, while initiators can be removed.

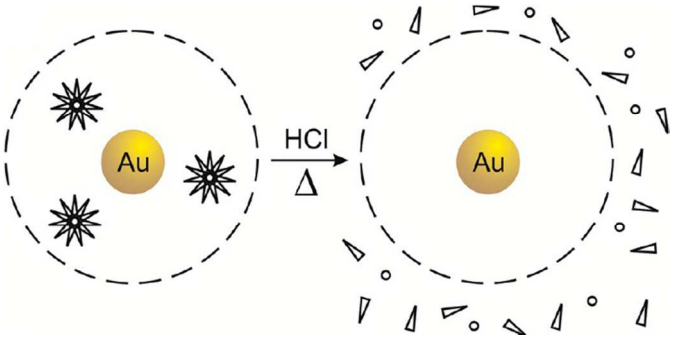

Fig. 15b Acid-promoted hydrolysis of the initiators, β-CD or TA. Hydrolysis products are released from nanocapsules where they were present.

Chen *et al.*[159] prepared cost effective Co@SiO_2 nanorattles as a mixture of hcp-Co and fcc-Co phases. This catalyst acts very efficiently to increase the rate of nitrophenol reduction and also has a very high stability.

Yun and coworkers[160] prepared a shell-in-shell structured nanocatalyst which is composed of mesoporous double TiO_2 and SiO_2 shell along with ultrafine Pd NPs uniformly distributed on the external and the internal surfaces of the meso-TiO_2 (@Pd/meso-TiO_2/Pd@meso-SiO_2). It contains an expanded surface area giving high catalytic activity. Mesoporous SiO_2 (meso-SiO_2) improves the stability of nanocatalysts[161,162] by resisting aggregation of active metal species. Decrease of leaching of the noble metals, improvement of accessibility of the active species and selectivity of reactants can be changed by altering the pore size whereas hydrophilicity or hydrophobicity can be changed by changing the surface[163,164] of the meso-SiO_2. The nanocatalyst is synthesized by initially coating SiO_2 with TiO_2 spheres by a sol-gel process, followed by etching of SiO_2 with NaOH giving @TiO_2 sphere which is then modified with -NH_2 groups using (3-aminopropyl)triethoxysilane (APTES) bestowing upon it a hydrophilic surface. Thereafter a Pd^{2+} ion diffusion process is applied which diffuses the Pd^{2+} directly into the central cavity of the @TiO_2, thereby forming a layer in the internal and external surface. It was then coated with resorcinol formaldehyde (RF) and meso-SiO_2 followed by calcination and reduction under hydrogen atmosphere. This is further utilised for the reduction of nitrophenol.

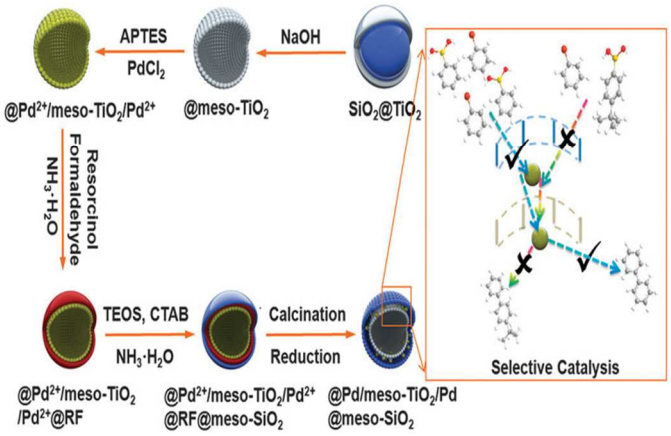

Fig. 16 Illustration of the synthesis of ''shell-in-shell'' @Pd/meso-TiO_2/Pd@meso-SiO_2 nanocatalyst.

Zhao *et al.*[165] synthesized highly ordered mesoporous silica in acidic THF/H_2O mixture using the template of poly(ethylene oxide)-*b*-poly(methyl methacrylate) (PEO-*b*-PMMA) and tetraethylorthosilicate (TEOS) as the silica precursor and utilising solvent evaporation induced aggregating assembly method (EIAA). While the THF is continuously evaporated from the solution, the template[166-168] along with the silica oligomer formed composite micelles and further formed large ordered face centered cubic mesostructures by assembling. Using *in situ* reduction method uniform gold nanoparticles can be introduced into the pores of the mesostructure which can act as an efficient catalyst for the reduction of nitrophenol with $NaBH_4$.

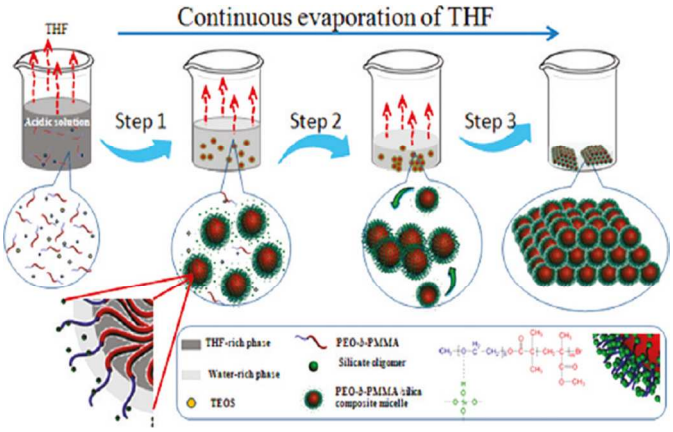

Fig. 17 Step 1: formation of the hybrid PEO-b-PMMA/SiO2 spherical micelles with PMMA core and silica-associated PEO shell by evaporating THF. Step 2: packing of the uniform hybrid micelles inside closed-packing fcc mesostructure on the interface of poor solvent water-rich phase, which is driven by the constantly increasing concentration of the composite micelles and the minimization of interface energy. Step 3: acceleration of cross-linking and condensation of the silicate oligomers for fixing the ordered mesostructure, which is formed due to the increased acidity of the reaction solution caused by evaporation of THF further.

Dendrimer[169-172] and micelle encapsulated metal nanoparticles have also been reported as catalyst for nitrophenol reduction. Kim *et al.*[173] reported gold nanoparticles using double hydrophilic block copolymer (DHBC) like polyethylene oxide-block-poly acrylic acid (PEO-block-PPA) as a template. Selective coordination between gold precursor and PAA block of the DHBC form micelle which are eventually converted to Au nanoparticles by using $NaBH_4$ as reducing agent. The DHBC–templated Au NPs was stable in water for months together without any significant aggregation. It showed improved catalytic activity for nitrophenol reduction due to the shell of DHBC which not only provides a confined interior but also acts like a template shell for the formation of spherical Au NPs. The nitrophenol reduction was carried out by $NaBH_4$ in the presence of the prepared catalyst.

Maleczka Jr. *et al.*[174] prepared nanoparticles from Pd(II) acetate or Pd/C, aqueous potassium fluoride, and polymethylhydrosiloxane (PMHS). This combination acted as an efficient catalyst to reduce nitro- substituted arenes and heteroarenes to their amines in high yield. On replacing the PMHS/KF with triethylsilane (Et_3SiH) the catalyst efficiently reduces aliphatic nitro to their hydroxylamines. Fluoride was important as it aids the formation of

polycoordinate siloxane intermediate for the facile transfer of hydrogen. These silanes and siloxanes helped to reduce nitroarene to aminoarene with $Pd(OAc)_2$/KF aq/THF and PMHS at room temperature. Bulky group on both ortho positions to nitro slowed down the reaction. Though electron withdrawing group and electron donating groups were well tolerated 4-nitrothioanisole was exceptional probably due to the scavenging nature of S towards Pd and a potential poison. 4-nitro benzaldehyde reduction was favoured highly but it also afforded reduction of aldehyde to alcohol. Sluggish reactivity was observed in case of 2 and 3-nitrobenzonitriles which could be reduced under forcing conditions but 4-nitrobenzonitrile stopped at N-hydroxylamine probably due to increased resonance stabilization of the intermediates. Nitro reductions failed in the presence of aromatic bromide and chloride whereas aromatic bromide and aliphatic bromide were not dehalogenated under this condition.

Nagashima *et al.*[175] proposed that Pt and Pd nanoparticles on three types of carbon nanofibres (CNF), such as those where the graphite layers are either perpendicular (platelet: CNF-P) or are parallel (tubular: CNF-T) or are stacked obliquely (herringbone: CNF-H), can be utilised as catalyst for reduction of arenes and functionalised nitroarenes selectively. A comparative study of the chemo selective reduction of the nitro group of chloronitrobenzene was carried out with solvents like ethyl acetate, hexane and ethanol, under varying H_2 pressure. Hetero atom containing compounds like n-octylamine, and different types of Pt or Pd combinations were also tried with CNF, at room temperature. The Pt/CNF-P combination was found to be the most efficient and reusable catalyst for the hydrogenation of nitroarenes to aromatic amines.

Patil *et al.*[176] prepared robust functionalised polymer like o-carboxymethyl chitosan (OCC) on which covalently bonded layer by layer self-assembled thin film of metal nanoparticle was formed. Metal nanocomposite was prepared *in situ* by the reduction of metal salts in polymer solution in the presence of hydrazine monohydrate. Quartz plate was then fabricated with OCC dried and further coated with polymer nanocomposite to form covalently bonded multi-layer thin film. These metal nanoparticles having different size, shape, polymeric matrix, deposition technique and total surface area have different catalytic activity in the reduction of 4-Nip to 4-Amp with sodium borohydride. The 10 layer films showed higher catalytic activity but less stability with respect to 20 or 40 layers, due to higher surface area of the porous membrane and the easy adsorption of the substrate and reducing agent.

He *et al.*[177] prepared robustly immobilized silver nanoparticles on porous bio-scaffolds like natural egg shell membrane at room temperature. Procyanidine, a polyphenol was used as a reductant and a stabilizer during synthesis. The reduction of 4-Nip, 2-Nip and 4-nitroaniline was carried out using $NaBH_4$ as the reducing agent.

Na *et al.*[178] prepared multifunctional and recollectable carbon nanotube ponytails (CNPs) by integrating CNT's into micrometer-sized colloidal particles. These CNPs act as catalyst for the reduction of 4-Nip to 4-Amp in the presence of $NaBH_4$.

Wang *et al.*[179] prepared monodispersed Ag nanocrystals in a one pot manner using as-prepared thiol functionalised bromide i.e. 1-(10-mercaptodecyl)-3-methyl-imidazolium bromide ([SH-C_{10mim}]Br) as a stabilizer. $AgNO_3$ was reduced by $NaBH_4$ in an aqueous solution of [SH-C_{10mim}]Br. The multipurpose ligand plays the important role of enhancing the catalytic property of the nanocrystal for the reduction of 4-Nip.

Byun *et al.*[180] in their work has synthesized Au nanoparticles by photochemical reduction in the presence of trisodium citrate under solar simulated light source which represents sunlight at room temperature. These gold nanoparticles were embedded physically on the filter paper and used for heterogeneous catalytic activity in the reduction of 4-Nip under the irradiation of the solar simulated light, and the reduction was due to photothermal heating property of Au nanoparticles.

Ramaraj *et al.*[181] prepared gold nanoparticles at room temperature and reduced with sodium citrate and $NaBH_4$. It was then supported on organic gel of phloroglucinolcarboxylic acid-formaldehydye (PF) gel. This was successfully used as catalyst for the reduction of 4-Nip.

Core shell particles both concentric[182] and eccentric[183] and also recyclable have been reported. Wang *et al.*[184] prepared in a one pot manner bimetal-nanoparticle-graphene hybrids of noble metals like Ag@Au and Ag@Pd as core shell by dc sputtering at room temperature. The as-prepared nanocatalyst has been used in the reduction of 4-Nip and its activity was enhanced with respect to monometallic hybrids due to modification of electronic structure and irregular morphology.

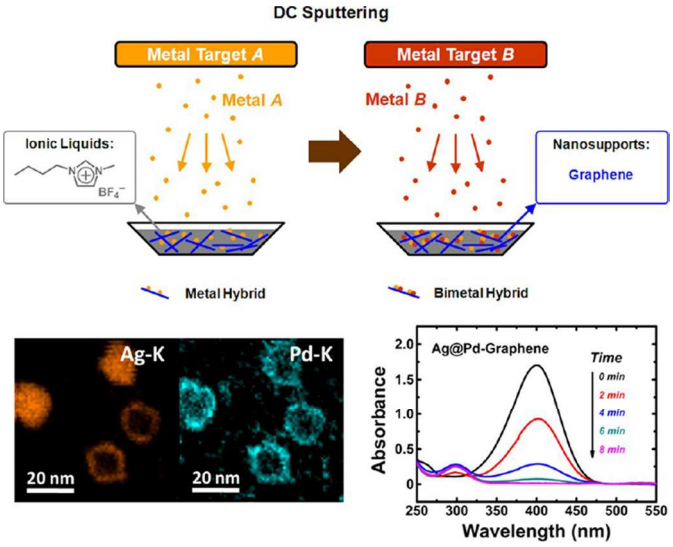

Fig. 18 Illustration of the synthetic procedure for Bimetal-NP-Graphene hybrids by sputtering metal A followed by sputtering metal B in room temperature ionic liquids where graphene is predispersed in absence of additives or byproducts.

Chen et al.[185] prepared Pd nanowire array catalyst from $PdCl_2$ in hydrothermal process by reducing it in the pores of

anodic aluminium oxide[186] templates with aluminium sheets behind, which not only reduces the Pd^{2+} ions to metal nanowires but also support them. This as-prepared catalyst can be further used for the reduction of 4-Nip and it has the property of repeatability.

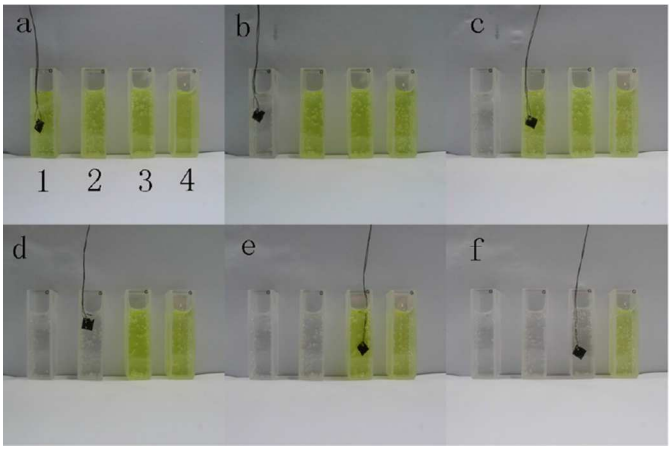

Fig. 19 Photos of recycled 4-Nip reduction process. (a) Cuvette 1 with beginning of the reaction. (b) Cuvette 1 with end of the reaction. (c) Cuvette 2 with beginning of the reaction (d) Cuvette 2 with end of the reaction. (e) Cuvette 3 with beginning of the reaction. (f) Cuvette 4 end of the reaction in. Cuvette 4 has the control sample.

Xu *et al.*[187] prepared SiO_2 supported immobilized polyvinylpyrrolidone (PVP) encapsulated Au nanoparticles. This was then treated with ultraviolet ozone to remove PVP stabilizer to various degree and further used to study the catalysis of the hydrogenation of p-chloronitrobenzene(p-CNB) and cinnamaldehyde (CAL) due to the gradual removal of PVP from the Au NPs. It was observed that Au NP decorated with stabilizer[188] acts as an excellent catalyst for the hydrogenation of p-CNB whereas it has a reduced activity for the hydrogenation of CAL. The activity for CAL increases with removal of stabilizer to various degrees.

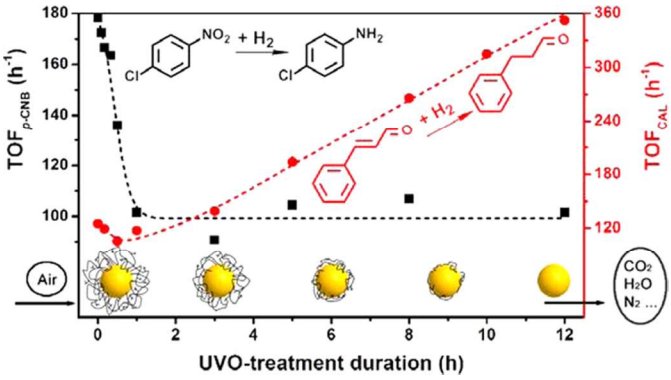

Fig. 20 Ultraviolet ozone removal of stabilizer around the gold nanoparticle to various degree resulting in variable efficiency of the catalyst for reduction reactions.

Bimetals have also been prepared for the partial reduction of nitrophenol for example AgPt[189] bimetal. Recently an article was published by Hou *et al.*[190] on star shaped Au-Cu alloy where synergy of both the metals has been studied by shape control. Tuneable size, pentacle, bimetallic gold copper alloy nanocrystals have been prepared by aqueous method which showed remarkable catalytic power for nitrophenol reduction with sodium borohydride. Growth showed a gradual modification of decahedral core to protruding branches along the twining planes.

Metal Oxide

Though most of the nitrophenol reduction has been made possible with costly metals like Pd and Pt but Chen *et al.*[191] had introduced cost effective metal oxides like Fe_3O_4@graphene oxide for the reduction of nitroarenes. Graphene oxide (GO) was obtained by exfoliation from Graphite Oxide which is prepared by Hummers Method.[192,193] GO, $FeCl_3.6H_20$ and $FeSO_4.7H_2O$ was treated at 68°C at pH 10. By ultrasonicating Fe_3O_4@GO composite was obtained which was separated with a permanent magnet. A comparative study was carried out for the reduction of nitro benzene without catalyst, with Fe_3O_4 NP and with Fe_3O_4@GO nanocomposite. A particular redox mechanism[194,195] was followed for the reduction of nitrobenzene over the Fe_3O_4@GO composite. The catalyst Fe^{3+} was reduced by hydrazine to Fe^{2+} while hydrazine decomposed to N_2 and H^+. The nitrobenzene was reduced to aniline by Fe^{2+} and H^+, while Fe^{2+} was oxidized to Fe^{3+}.

In another work Siadatnasab *et al.*[69] had demonstrated the preparation of NiO nanoparticle from bis(dimethylglyoximato)Nickel(II)complex ($Ni(dmgH)_2$) by heating in an electric furnace at 400°C in air. Here the nitroarene was added to KOH, ethanol and NiO was taken as catalyst and irradiated in laboratory microwave oven at 180W. This reduction was monitored by TLC and GC-MS. The reaction was alternatively tried in reflux, in an oil bath. In the absence of NiO and KOH no reaction took place. H-donors like methanol, 1-propanol, 2-propanol, 2-butanol and tert-butanol was used and it was found that apart from ethanol only 2-propanol was effective. KOH and NaOH had comparable reactivity whereas $Ca(OH)_2$ and Na_2CO_3 yielded lesser amount of aniline as its basicity is lower than KOH. However, Me_3N and NH_3 did not yield any product. This was studied for most of the nitro arenes having electron donating and electron withdrawing substitutions.

Swaminathan *et al.*[196] in his work had made Ag-TiO_2 by facile photodeposition where the TiO_2 is in the anatase phase. TiO_2 nanoparticle was prepared from titanium tetraisopropoxide in isopropanol solution which was a colloidal suspension. Silver nitrate was the silver source which was added in the TiO_2 suspension at pH 3 and then irradiated with UV light to yield Ag-TiO_2 catalyst.[197] They investigated the reduction of nitro group to amine followed by condensation with aldehyde to give a cyclic quinaldine.

Kiasat *et al.*[198] in their experiment for the reduction of nitroarene used rice husk-SiO_2-aminopropylsilane composite as catalyst. They extracted silca from rice husk (RH). In order to prepare rice husk propylaminesilane ($RHPrNH_2$) the nanosilica was stirred with NaOH, filtered and treated with nitric acid to form a gel. $RHPrNH_2$ was then dispersed in freshly prepared NaBH4 in ice bath and then $AgNO_3$ solution was added at room temperature to prepare silver immobilized $RHPrNH_2$ ($RHPrNH_2$@Ag). To reduce the nitroaromatic compound $NaBH_4$ was added along with catalyst at room temperature. Then water was added and the suspension was kept in reflux under stirring condition. The completion was detected with TLC (Et_2O/n-hexane as eluent: 1/5).

Kappe *et al.*[199,200] used hydrazine hydrate ($N_2H_4.H_2O$) as reducing agent and stabilized colloidal iron oxide (Fe_3O_4) nanocatalyst to selectively reduce nitroarenes to aniline. Fe_3O_4 was prepared from Fe precursors with hydrazine hydrate in known procedures[201,202] using small-scale microwave batch heating at elevated temperature. The reduction of nitrobenzene was carried out with Fe precursors like tris(acetylacenato)Iron(III) [$Fe(acac)_3$], $FeCl_2.4H_20$, $FeCl_3.6H_2O$ and $Fe(OAc)_2$ as catalyst and hydrazine in methanol as the reducing agent in microwave. Fe_3O_4 nanocrystals were generated *in situ* and it was efficient in catalysing nitrobenzene reduction. Dehalogenation of -chloro, -bromo or -iodo substituted nitrobenzene did not take place even in high temperature. Selective reduction of functionalised nitroarene was obtained which is of great importance in organic synthesis.

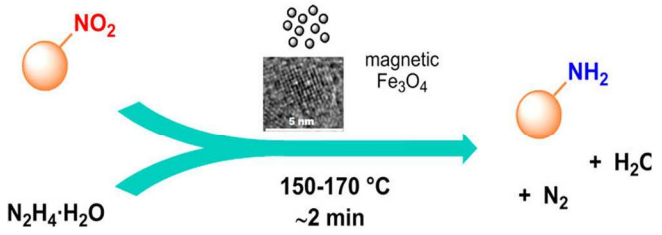

Fig. 21 Iron oxide nanoparticles generated *in situ* which can be utilised for nitroarene reduction using continuous flow method.

Nitro compound reduction being a novel method to test the efficacy of a catalyst particle Keane *et al.*[203] carried out selective gas phase hydrogenation of p-chloronitrobenzene (p-CNB) to p-chloroaniline using H_2 gas as the reducing agent along with Mo_2N and Au/Mo_2N as the catalyst. Alfa Aesar was taken as a MoO_3 precursor and Mo_2N was prepared via temperature programmed treatment in H_2/N_2 or H_2/N_2/Ar continuous flow at atmospheric pressure. First β-Mo_2N and γ-Mo_2N was synthesised and then Au/Mo_2N preparation was carried using $HAuCl_4$ solution.

Bokhoven *et al.*[204] studied the one pot reaction with nitrobenzene using Au@TiO_2, mesitylene and ethanol with Ar purged condition. The catalyst was prepared using TiO_2, $HAuCl_4$ and urea at 60°C. It was pre-treated in hydrogen atmosphere (H_2/He) at 60°C.

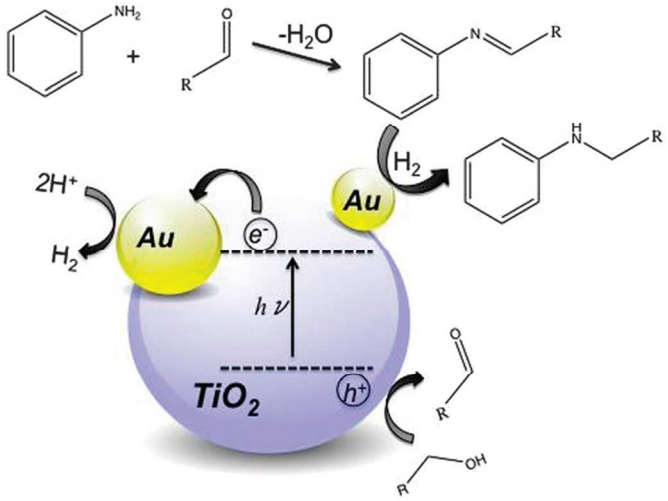

Fig. 22 Proposed reaction mechanism for one-pot photo-reductive N-alkylation of aniline and nitroarene with primary alcohols using Au–TiO_2 nanoparticle as catalyst.

Some hollow metal nanocomposite can be prepared to utilise directly as a metal catalyst or hollow nanostructures[205] can be modified to encapsulate[206-209]metal nanoparticles which can be utilised as catalyst for nitroarene reduction.

Hyeon *et al.*[210] prepared magnetically recyclable[211] hollow nano composite by reacting $FeCl_3.6H_2O$ with sodium dodecyl sulfate solution, and adding $PdNO_3$ hydrate and pyrrole to it under high temperature and H_2 gas flow. This nanocomposite was then used to load other noble metal catalyst like Rh to reduce selectively the nitro group in presence of halogen of substituted nitro benzene with hydrazine as reducing agent at elevated temperature.

Fig. 23 Heterogeneous reduction of nitrobenzene with hydrazine using magnetically recyclable hollow nanocomposite catalysts. Catalyst separated by a magnet kept in contact with the bottle from outside.

In the work of Ranu *et al.*[212] spherical Fe(0) nanoparticle was made from $FeSO_4.7H_2O$ using $NaBH_4$ in presence of citric acid at room temperature. The catalyst so produced could not be activated in toluene, methyl chloride, N,N-dimethylformamide or dry methanol but was activated in water to selectively reduce the substituted nitro arenes. The reaction proceeds by the formation of -NO, -NHOH and -

N=N(O)- . During the reaction speherical Fe(0) was transformed to Fe_3O_4 nanotubes.

Su *et al.*[213] used one pot surfactant free hydrothermal method to synthesise γ-Fe_2O_3-polymer porous composites using iron acetyl acetonate followed by polymerisation with formaldehyde in alkaline medium at 160°C. Hydrazine hydrate in presence of catalyst in ethanol at 85°C reduces nitrophenol to nitroaniline. Compared to the commercial γ-Fe_2O_3, α-Fe_2O_3 and Fe_3O_4, the as-synthesised catalyst has a higher yield due to the increased surface area of the porous composites.

Bhaumik *et al.*[214] made NiO-Al_2O_3 mixed oxide nanocomposite using lauric acid as capping agent containing high surface area and high mesoporosity which rendered to be an effective catalyst for region-selective reduction of nitro group of nitroarenes using liquid phase hydride transfer reactions where 2-propanol acts as the hydride source. More activated aromatic rings like 4-chloro nitrobenzene are reduced faster whereas deactivated ring like m-dinitrobenzene are slower in getting reduced. In absence of catalyst the reaction do not take place, on adding Al catalyst the reaction becomes very slow, only with Al-Ni catalyst the reaction is fast hence Ni(II) plays a vital role in reduction as revealed by us in our work with Pt-Ni.[122]

Teodoro *et al.*[215] made magnetic ferrite-nickel (Fe_3O_4-Ni) nanoparticle by wet impregnation method followed by chemical reduction. With this nanocomposite the nitrophenol reduction was carried out using glycerol as the solvent and hydrogen donor. On studying the reduction with differently substituted nitro compounds it was observed that due to bulky nature of the catalyst the yield decreased for ortho-substituted nitro compounds but not significantly.

Kappe *et al.*[216] had prepared magnetic Fe_3O_4 catalyst nanoparticle *in situ* from iron salts. The Fe precursor was added to the reaction mixture containing hydrazine hydrate and nitroarene and heated in a microwave at 150 ºC to give chemoselective reduction of substituted nitroarenes. Alcohols like methanol, ethanol and 2-propanol gave significant reduction whereas in acetonitrile and water the yield decreased significantly which could be improved at high temperature.

Tilve *et al.*[217] used Cu(II) bromide as the procatalyst for *in situ* production of highly active Cu nanoparticles along with Cu_2O which formed due to atmospheric oxidation. The reaction was then attempted with CuO and Cu_2O but gave no yield. Methanol and ethanol were found to be the best solvent. This reduction with $NaBH_4$ was accompanied with reduction of aldehyde to alcohol, CN to benzyl amine and reduction of allylic conjugated double bonds, however aliphatic nitro group was unaffected.

Study on the interaction of aromatic rings with metal surface depending on the potential of the aromatic rings and the facets of the metal crystals has been reported.[3] We have prepared CuO-MnO_2[218] composite nanostructures from time-dependent redox transformation between Cu_2O and $KMnO_4$. After transformation the structures resemble the parental structure but becomes porous in nature which on prolonged reaction time ruptures to tiny spherical porous nanocomposite which has the highest catalytic activity. These nanocomposite show well defined facet-dependent nitroarene reduction with $NaBH_4$. Depending on the surface area and the porosity, the order of catalytic activity was as follows, the tiny spherical CuO-MnO_2 >octahedral CuO-MnO_2(111) > cubic CuO-MnO_2 (100) > spherical CuO-MnO_2 > octahedral Cu_2O(111) > cubic Cu2O (100) > spherical Cu_2O > CuO > MnO_2. Reduction of nitro group of nitroarenes in the presence of functional groups like -CH_3, -CHO, -COMe, -NHCOMe, -COOH have been studied extensively.

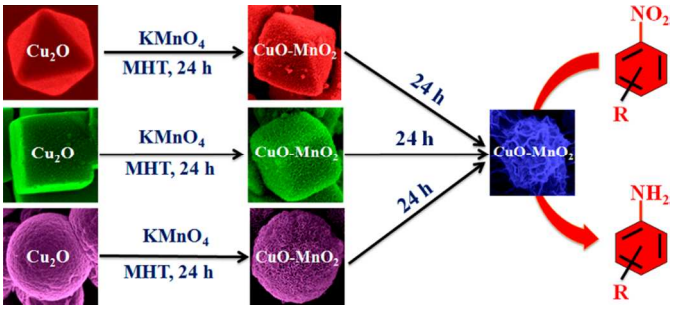

Fig. 24 Facet dependent reduction of nitrophenol with CuO-MnO_2 nanocomposites.

Now an upcoming area has become a hot topic in the catalysis world and that is heterojunction within catalyst particles.

Priestley *et al.*[219] prepared multilaminated ZnO/TiO_2 films with heterojunction, which were deposited layer by layer from oxide colloids in absence of polyelectrolytes, on conductive substrates like fluorine-doped tin oxide glass and indium tin oxide coated poly(ethylene terephthalate).

Zhang *et al.*[220] prepared hollow mesoporous nanosphere of M/CeO_2 (M=Au, Pd, and Au-Pd) which was synthesised with desirable size, shell thickness, and dispersion of noble metal nanoparticles. These nanocatalysts were effectively used in nitrophenol reduction.

Metal Sulfide

As reported earlier in the semiconductor mechanism Pradhan *et al.*[101] prepared capped ZnS quantum dots (ZnS QDs) as sol and used it to reduce nitrophenol under UV-light in the presence of $NaBH_4$. On increasing the carbon chain of the cap the reaction rate decreases. Again, when ZnS was doped with Mn or Cu this reduction was either stopped or proceeded at slow rate, respectively. On studying ZnSe, CdS and ZnTe the reduction occurred in the first case but not in the other two cases. In actual experimental procedure the authors have impressed upon the effect of capped semiconductor ZnS QDs for UV light (254 nm) mediated nitrophenol reduction and surprisingly concluded that similar reduction is true for simple nanocrystals also.

Supported metal and metal oxide

Innumerable work have been reported on graphene based materials.[221-224]

We for the first time reported the immobilization of gold[225] nanoparticles in anion exchange resin which could be retrieved quantitatively by cationic surfactant, cetylpyridinium chloride. This resin supported gold nanoparticle could be utilised as solid phase catalyst for the reduction of 4-Nip with $NaBH_4$. On completion of the reduction process the solid matrix remained activated and yet separated from 4-Amp which was the product. The gold particles could also be recovered from the resin support with unaffected particle morphology.

Kim *et al.*[226] prepared hybrid gold nanoparticle-graphene oxide (Au-GO) nanosheets through electrostatic self-assembly. By this method effective concentration of active Au-nanoparticle on the graphene sheet could be controlled and there also existed a synergistic catalytic activity of the Au and GO. Nitrophenol reduction was carried out with the hybrid catalyst and $NaBH_4$ as the reducing agent. Conversion of 3-nitroaniline was the most efficient with this catalyst. Substrate like secondary amines or imines were formed more efficiently than benzyl alcohol. They also prepared silver nanoparticles[227] which formed spontaneously on graphene oxide nanosheets functionalised with mussel-inspired dopamine (GO-Dopa) without any reductant or stabilizer at room temperature. The hybrid Ag/GO-Dopa displayed excellent catalytic activity in the reduction of a series of nitroarenes regardless of the types and positions of the substituent.

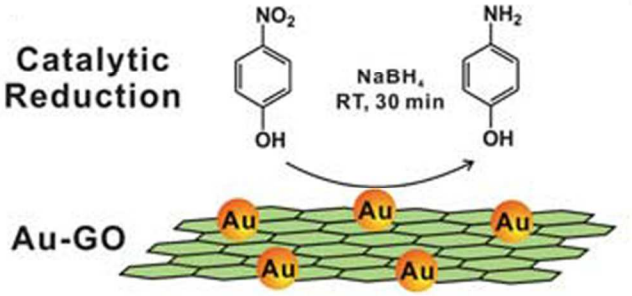

Fig. 25 Illustration of electrostatic self-assembly of nanoparticles on GO nanosheet and its catalytic activity in nitrophenol reduction.

Chen *et al.*[228] prepared magnetically separable Ni_xCo_{100-x} (x = 0, 25, 50, 75, and 100) which was grown in reduced graphene oxide nanosheets. The nanocomposite was used to reduce 4-Nip to 4-Amp in the presence of $NaBH_4$. RGO-Ni_xCo_{100-x} shows higher catalytic activity with respect to NixCo100-x, and RGO-$Ni_{25}Co_{75}$ gives the best result. The adsorption of the substrate on RGO was due to π-π stacking interaction alone or its combined effect with the charge transfer between Ni_xCo_{100-x} nanoparticles.

Qui *et al.*[229] prepared Cu_2O on two-dimensional boron nitride (h-BN)[230-238] nanosheets as supporting substrate. The octahedron structure of Cu_2O anchors on the h-BN sheets due to the –OH and –NH- groups present. The formation and adsorption of the phenolate ion is initiated by the h-BN component of the composite and the Cu_2O transfers hydrogen and electrons from the borohydride ions to the nitrophenol and reduce it to aminophenol.

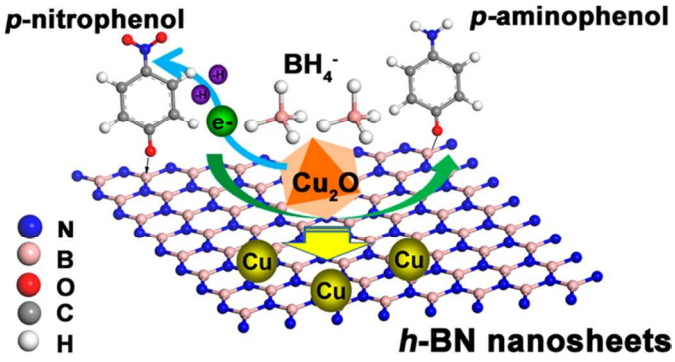

Fig. 26 Schematic of the anchoring of Cu_2O on the h-BN nanosheets thereby aiding in the reduction processs.

Another group of scientists, Chen *et al.*[239] prepared a nanocomposite of Cu nanoparticles on reduced graphene oxide by using hydrazine at room temperature. 4-Nip reduction was carried out by this nanocomposite at temperature varying from 25-40 ºC.

Ma *et al.*[240] in their work have modified fibrous dandelion-like nano-silica (KCC-1) functionalised with mercaptopropyltriethoxysilane groups and containing Ni@Au core-shell nanoparticles anchored on the fibers. Au seeded Ni nanoparticle was prepared which served as the core. This showed superior catalytic property on 4-Nip reduction to 4-Amp in the presence of $NaBH_4$.

Banerjee *et al.*[241] prepared a stable supramolecular hydrogel of graphene oxide in presence of polyamines forming cross linked nanosheets using base electrostatic interaction. Upon addition of a mild reducing agent, like vitamin C, an *in situ* reduction of graphene oxide sheets within the hydrogel matrix takes place. Noble metal containing reduced graphene oxide based hybrid hydrogels were prepared by *in situ* co-reduction of GO and metal precursor. The metal uniformly distributed on the RGO-based hybrid hydrogel matrix which acts as a catalyst for aromatic nitro group reduction. On reducing 4-Nip and p-nitroaniline in the presence of $NaBH_4$ a decrease in the UV-Vis absorption was noted in the latter case with the as-synthesized nanoparticle containing hybrid hydrogel matrix.

Murata *et al.*[242] prepared dispersed gold nanoparticle using DNA[243-250] cross-linked hydrogel as the matrix. These are some of the smallest gold nanoparticles reported considering in-gel metal nanoparticles. DNA hydrogel films were incubated with $HAuCl_4$. The film was treated with $NaBH_4$ to reduce Au(III). $NaBH_4$ was used along with the hydrogel to give aminophenol from nitrophenol.

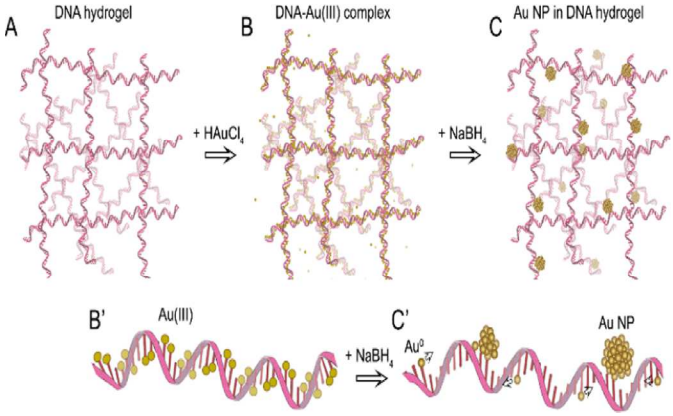

Fig. 27 Illustration of Au(III) reduction in DNA hydrogel matrix and formation of nanoparticles which in turn locally binds to DNA. (A) The DNA hydrogel. (B and B) The DNA complex with the Au(III) complex. (C and C) Au nanoparticles bound locally to the DNA scaffold of hydrogel.

Another group, Chen *et al.*[251] prepared Au nanoparticle on SiO_2/poly(2-(dimethylamino)ethyl metharylate) brushes which was also used as catalyst for nitrophenol reduction.

Gold nanoparticle was prepared using CO_2-switchable polymers by Ma *et al.*[252] as well, using poly(N,N-dimethylaminoethylmethacrylate). This was also used for the nitrophenol reduction.

Lykakis *et al.*[253] prepared mesoporous titania supported gold nanoparticle assemblies [Au/MTA(x)(x=0.5, 1, and 2)] which can catalyze, x=2 being the most efficient, the activation of $NaBH_4$ for the reduction of nitroarenes to corresponding anilines in moderate to high yields, whereas nitroalkanes can be reduced to the corresponding diazo-, and hydrazo-compounds. Nitrotoluene was treated with $NaBH_4$ and ethanol to give 4-toluidine. However in the presence of NaH, $LiBH_4$, BH_3-THF hydrides no conversion was noted, neither was any reaction observed with THF only. The role of protic solvent in the presence of EtOAc, THF and CH_3CN along with a small amount of water was essential for the reduction procedure.

Liu *et al.*[254] prepared highly dispersed palladium nanoparticles on mesoscopic carbon porous material (CPM) by microwave irradiation using soft templating approach with palladium(II)acetylaetonate as the metal precursor and phloroglucinol and formaldehyde as primary carbon precursor. The nanocatalyst was used for 4-Nip reduction to 4-Amp with $NaBH_4$ as reducing agent.

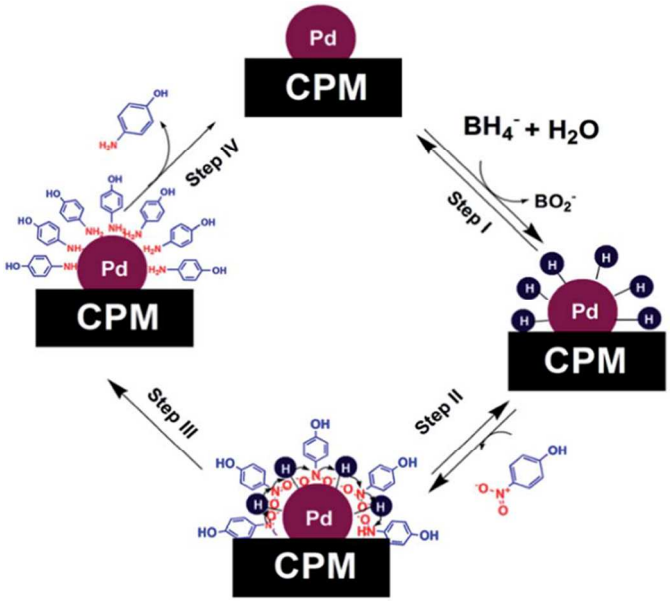

Fig. 28 Illustration of the mechanism of the reduction of 4-Nip by $NaBH_4$ using Pd/CPM as catalyst.

Banerjee *et al.*[255] prepared immobilized Au nanoparticle in stable covalent organic framework (COF) using solution infiltration method. $HAuCl_4.3H_2O$ was taken as the precursor for gold along with evacuated TpPa-1 and methanol, and stirred vigorously.[256] $NaBH_4$ was used as the reducing agent for the formation of Au(0)@TpPa-1 which contained a stable COF consisting of ordered porous architecture with a crystalline framework enriched with oxygen and nitrogen which in turn provide stability to the nanoparticle. This nanocatalyst was further used to catalyze nitrophenol reduction with $NaBH_4$.

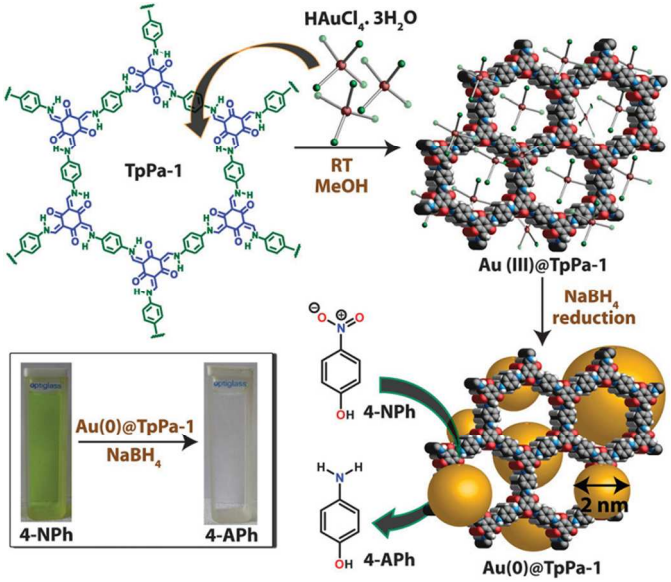

Fig. 29 Illustration of the synthesis of Au(0)@TpPa-1 catalyst using solution infiltration method to reduce nitrophenol. Inset image: The images of the colour change observed due to the conversion of 4-Nip to 4-Amp after the addition of Au(0)@TpPa-1.

Xu *et al.*[257] prepared immobilized Au@Ag core-shell nanaoparticles on a metal organic framework[258] (MOF) by sequential deposition-reduction method. Size of the Au@Ag elucidates the restricted pore/surface structure in the MOF. The Au/Ag ratio was modulated to tune the composition and a reversed sequence of Au/Ag deposition changed the structure of Au-Ag nanoparticles to AuAg alloy. Catalysis of 4-Nip reduction reveal a strong bimetallic synergistic effect of the core shell structured Au@Ag NPs which are better catalyst than the alloy or monometallic nanoparticles.

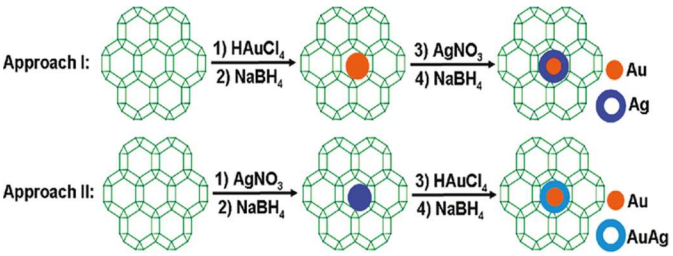

Fig. 30 Illustration of the synthetic strategies.

Muller *et al.*[259] prepared one dimensional silica nanostructures which were uniform with tunable dimension and morphology using core degradable core-shell cylindrical polymer brushes (CPBs) as template. The polymer core-shell was made up of densely grafted poly(ε-caprolactone) core and a poly[2-(dimethylamino)ethyl methacrylate] (PDMAEMA) shell. Varied degree of polymerization of the backbone and the side chain of the silica results in varying lengths and diameters of the silica nanostructures. These silica hybrids when treated with acid or calcined gave hollow silica nanotubes. Metal salts like Pt and Au can be doped in the silica hybrid nanowires which can be further accessed as catalyst for reduction of 4-Nip to 4-Amp.

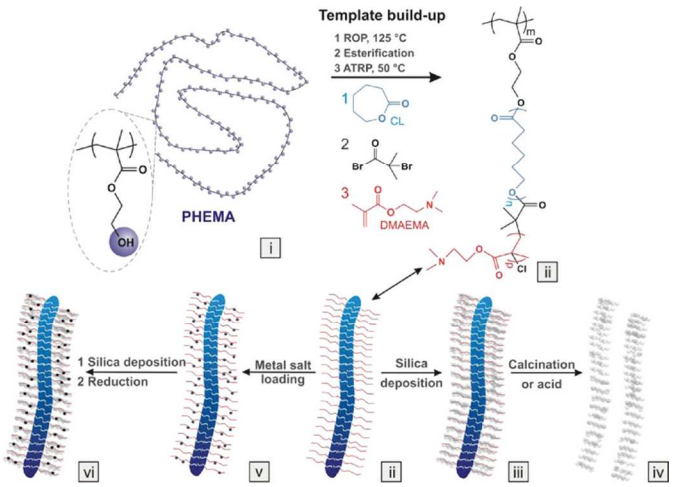

Fig. 31 Schematic of the synthesis of silica nanotube with core degradable core-shell.

Zhang and coworkers[260] prepared uniform pomegranate like $Pt@CeO_2$ multicore@shell nanosphere using clean nonorganic synthetic method. The redox reaction involved the precursor $Ce(NO_3)_3$ and K_2PtCl_4, in an alkaline aqueous solution, in the absence of any reducing agent or surfactant in Ar atmosphere. The $Pt@CeO_2$ multicore@shell nanosphere was also supported on reduced graphene oxide which could be utilised for the catalysis of nitrophenol reduction.

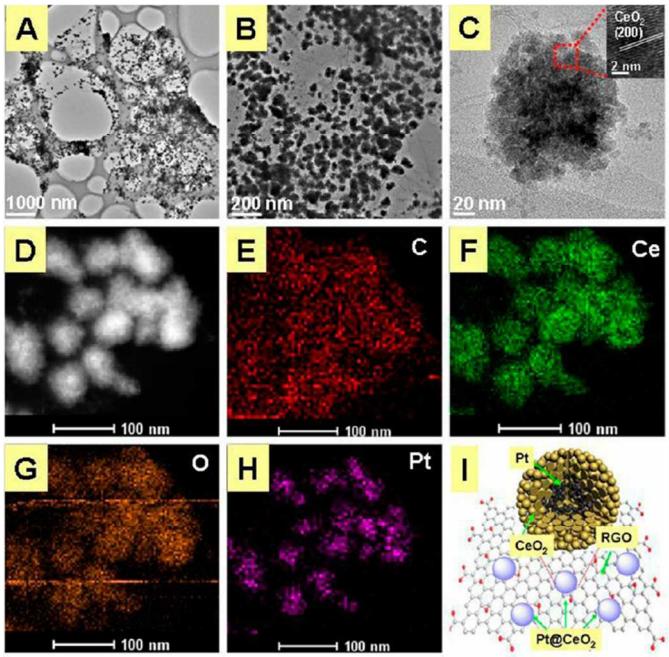

Fig. 32 (A–C) The TEM images of Pt@CeO2/RGO hybrid nanocomposites. (D) The corresponding STEM images. (E: carbon; F: cerium; G: oxygen; and H: platinum) The EDX mapping analysis. (I) The structure diagram of the Pt@CeO2/RGO catalyst.

Li *et al.*[261] prepared redox active Cu(I)boron imidazolate framework (BIF) which has a ladder–chain structure and exhibit mechanochromic luminescence. Due to its rich B-H functional bonds in its structure it can reduce Ag nanoparticle. The Ag@BIF-34 has higher catalytic activity towards nitrophenol reduction in comparison to BIF-34.
Jung *et al.*[262] composed novel zeolite L-mimic-organic framework (ZLMOF) which were tubular in structure. This when treated with $AgBF_4$ at 40°C smoothly coated the surface of the ZLMOF with Ag(0) nanoparticles yielding Ag(0)/ZLMOF which had higher catalytic activity than ZMLOF alone for nitrophenol reduction with $NaBH_4$.

MNps have long (over 150 years) been studied, beginning with the Royal Institute, London, when Michael Faraday produced a 'hydrosol' of gold for the first time in the year 1857. Now, MNps can be tested with a simple reaction in aqueous medium using only a visible spectrophotometer. Novel research based on the model nitroaromatic reduction are innumerable. The essence of this remarkable reaction emanated in the works of scientists all over the world.[263-265]

Enormous amount of work have been carried out by different laboratories which authenticate the success of the reaction to test a catalyst.

Conclusions

In this brief review we have circumvented the present status of testing metal and metal oxide catalyst particles in their nano regime using a simple novel reaction. The reaction is so chosen to suite any chemical laboratory using visible spectrophotometry. The isobestic point, reproducibility, kinetics all have to be accounted keeping an eye to the published mechanisms. Adsorption phenomenon that leads to product formation has also been described taking structural morphological faceted, precisely high index faceted, metal and metal oxide catalyst particles into consideration. Hope the future would be enlightened by the described model reaction.

Acknowledgements

T. Aditya is thankful to Dr. Anjali Pal and the other lab mates for helpful discussions and suggestions. We are thankful to all the reviewers for suggestions and constructive comments.

Notes and references

[a]Department of Chemistry, Indian Institute of Technology, Kharagpur 721302, India. E-mail: tpal@chem.iitkgp.ernet.in
[b]Department of Civil Engineering, Indian Institute of Technology, Kharagpur 721302, India.

1. K. Kuroda, T. Ishida and M. Haruta, *J. Mol. Catal. A: Chem*., 2009, **298**, 7.
2. J. He, I. Ichinose, T. Kunitake, A. Nakao, Y. Shiraishi and N. Toshima, *J. Am. Chem. Soc*., 2003, **125** , 11034.
3. C.-Yi Chiu, H. Wu, Z. Yao, F. Zhou, H. Zhang, V. Ozolins, and Y. Huang, *J. Am. Chem. Soc.,* 2013, **135**, 15489.
4. J. Kouz and R. S. Varma, *Chem. Commun*., 2013, **49**, 692.
5. A. Mitra, D. Jana and G. De, *Chem. Commun*., 2012, **48**, 3333.
6. H. Ye and R. M. Crooks, *J. Am. Chem. Soc*., 2007, **129**, 3627.
7. S. Panigrahi, S. Basu, S. Praharaj, S. Pande, S. Jana, A. Pal, S. K. Ghosh and T. Pal, *J. Phys. Chem. C*, 2007, **111**, 4596.
8. M. J. Vaidya, S. M. Kulkarni, R. V. Chaudhari, C. V. Rode, M. J. Vaidya and R. V. Chaudhari, *Org. Process Res. Dev.*, 1999, **3**, 465.
9. N. Comisso, S. Cattarin, S. Fiameni, R. Gerbasi, L. Mattarozzi, M. Musiani, L. Vazquez-Gomez and E. Verlato, *Electrochem. Commun*., 2012, **25**, 91.
10. K. B. Narayanan and N. Sakthivel, *J. Hazard. Mater*., 2011, **189**, 519.
11. T. L. Lai, K. F. Yong, J. W. Yu, J. H. Chen, Y. Y. Shu and C. B. Wang, *J. Hazard. Mater*., 2011, **185**, 366.
12. D. Makovec, M. Sajko, A. Selisnik and M. Drofenik, *Mater. Chem. Phys*., 2011, **129**, 83.
13. S. S. Kumar, C. S. Kumar, J. Mathiyarasu and K. L Phani, *Langmuir,* 2007, **23**, 3401.
14. J. Liu, G. Qin, P. Raveendran and Y. Ikushima, *Chem. Eur. J.,* 2006, **12**, 2131.
15. M. Zhang, L. Liu, C. Wu, G. Fu, H. Zhao and B. He, *Polymer* 2007, **48**, 1989.
16. B. Baruah, G. J. Gabriel, M. J. Akbashev and M. E. Booher, *Langmuir,* 2013, **29**, 4225.
17. Y. Gao, X. Ding, Z. Zheng, X. Cheng and Y. Peng, *Chem. Commun.,* 2007, 3720.
18. X. Chen, D. Zhao, Y. An, Y. Zhang, J. Cheng, B. Wang and L. Shi, *J. Colloid Interface Sci.,* 2008, **322**, 414.
19. M. H. Rashid and T. K. Mandal, *Adv. Funct. Mater.,* 2008, **18**, 2261.
20. J. Lee, J. C. Park and H. Song, *Adv. Mater.,* 2008, **20**, 1523.
21. A. Dandapat, D. Jana and G. De, *Appl. Mater. Interfaces,* 2009, **1**, 833.
22. S. Harish, J. Mathiyarasu, K. L. N. Phani and V. Yegnaraman, *Catal. Lett.,* 2009, **128**, 197.
23. Y.-C. Chang and D.-H. Chen, *J. Hazard. Mater.,* 2009, **165**, 664.
24. S. Behrens, A. Heyman, R. Maul, S. Essig, S. Steigerwald, A. Quintilla, W. Wenzel, J. Burck, O. Dgany and O. Shoseyov, *Adv. Mater.,* 2009, **21**, 3515.
25. M. A. Mahmoud, B. Snyder and M. A. El-Sayed, *J. Phys. Chem. Lett.,* 2010, **1**, 28.
26. K. Esumi, R. Isono and T. Yoshimura, *Langmuir,* 2004, **20**, 237.
27. H. Wu, Z. Liu, X. Wang, B. Zhao, J. Zhang and C. Li, *J. Colloid Interface Sci.,* 2006, **302**, 142.
28. Y. Wang, G. Wei, W. Zhang, X. Jiang, P. Zheng, L. Shi and A. Dong, *J. Mol. Catal. A: Chem.,* 2007, **266**, 233.
29. H. Zhang, X. Li and G. Chen, *J. Mater. Chem.,* 2009, **19**, 8223.
30. J. Zeng, Q. Zhang, J. Chen and Y. Xia, *Nano Lett.,* 2010, **10**, 30.
31. K. S. Chin, J.-Y. Choi, C. S. Park, H. J. Jang and K. Kim, *Catal. Lett.,* 2009, **133**, 1.
32. L. Shang, T. Bian, B. Zhang, Dr. D. Zhang, L.-Z. Wu, C.-Ho Tung, Y. Yin and T. Zhang, *Angew. Chem.*, 2014, **126**, 254.
33. M. A. Mahmoud, D. O'Neil and M. A. El-Sayed, *Chem. Mater.,* 2014, **26**, 44.
34. R. S. Dowing, P. J. Kunkeler and H. van Bekkum, *Catal. Today*, 1997, 37, 121.
35. M. Suchy, P. Winternitz and M. Zeller, World (WO) Patent, 91, 00278, 1991.
36. N. Pradhan, A. Pal and T. Pal, *Colloids and Surfaces A: Physicochem. Eng. Aspects*, 2002, **196**, 247.
37. K. Layek, M. L. Kantam, M. Shirai, D. N.-Hamane, T. Sasakid and H. Maheswarana, *Green Chem*., 2012, **14**, 3164
38. P. Veerakumar, M. Velayudhamb, K.-L. Lu and S. Rajagopal, *Appl. Catal. A: Gen.*, 2012, **439– 440**, 197.
39. T. R. Mandlimath and B. Gopal, *J. Mol. Catal. A: Chem*, 2011,**350**, 9.
40. S. Jana, S. Pande, S. Panigrahi, S. Praharaj, S. Basu, A. Pal, and T. Pal, *Langmuir*, 2006, **22**, 7091.

41. A. Gangula, R. Podila, R. M, L. Karanam, C. Janardhana and A. M. Rao, *Langmuir,* 2011, **27**, 15268.
42. D. Astruc, Nanoparticles and Catalysis, Wiley-VCH: New York, 2008, 1.
43. R. Narayanan and M. A. El-Sayed, *J. Phys. Chem. B,* 2005, **109**, 12663.
44. A. S. Hashmi and G. J. Hutchlings, *Angew. Chem., Int. Ed.* 2006, **45**, 7896.
45. D. Astruc, F. Lu and J. R. Aranzaes, *Angew. Chem., Int. Ed.* 2005, **44**, 7852.
46. S. Kundu, M. Mandal, S. K. Ghosh, and T. Pal, *J. Colloid Interface Sci.,* 2004, **272,** 134.
47. S. Pande and T. Pal, *J. Indian Chem. Soc*., 2010, **87**, 425.
48. J. Das, Md. A. Aziz and H. Yang, *J. Am. Chem. Soc*., 2006, **128**, 16022.
49. C. D. Pina, E. Falletta, L. Prati and M. Rossi, *Chem. Soc. Re*V., 2008, **37**, 2077.
50. J. Gong and C. B. Mullins, *Acc. Chem. Res.* 2009, **42**, 1063.
51. N. R.Shiju and V. V. Guliants, *Appl. Catal., A*, 2009, **356**, 1.
52. M. Haruta and M. Date, *Appl. Catal., A,* 2001, **222**, 427.
53. J. M. Campelo, D. Luna, R. Luque, J. M. Marinas and A. A. Romero, *ChemSusChem,* 2009, **2**, 18.
54. N. Pradhan, A. Pal and T. Pal, *Langmuir,* 2001, **17***,* 1800.
55. S. K. Gosh, M. Mandal, S. Kundu, S. Nath and T. Pal, *Appl. Catal. A: Gen.,* 2004, **268**, 61.
56. Y. Mei, Y. Lu, F. Polzer and M. Ballauff, *Chem. Mater.,* 2007, **19**, 1062.
57. T. Tanaka, A. Nakajima, A. Watanabe and T. Ohno and Y. Ozaki, *Vib. Spectrosc*., 2004, **34**, 157.
58. M. Erol, Y. Han, K. Scott, M. C. Stafford, H. Du, S. Sukhishvili, *J. Am. Chem. Soc.,* 2009, **131**, 7480.
59. M. Muniz-Miranda, *Appl. Catal. B: Environ,* 2014, **146**, 147.
60. T. Fu, M. Wang, W. Cai, Y. Cui, F. Gao, L. Peng, W. Chen and W. Ding, *ACS Catal*., 2014, **4**, 2536.
61. A. G. Majouga, E. K. Beloglazkina, E. A. Manzheliy, D. A. Denisov, E. G. Evtushenko, K. I. Maslakov, E. V. Golubina and N. V. Zyk, *Appl. Surf. Sci*., 2015, **325**, 73.
62. M. Brust, M. Walker, D. Bethell, D. J. Schiffrin and R. Whyman, *J. Chem. Soc., Chem. Commun*., 1994, 801.
63. N. S. Karan, D. D. Sarma, R. M. Kadam and N. Pradhan, *J. Phys. Chem. Lett.*, 2010, **1**, 2863.
64. S. P. Prakash and K. R. Gopidas, *ChemCatChem*, 2014, **6**, 1641.
65. S. Saha, A. Pal, S. Kundu, S. Basu and T. Pal, *Langmuir*, 2010, **26**, 2885.
66. S. Jana, S. Pande, A. K. Sinha and T. Pal, *Inorg. Chem*., 2008, **47**, 5558.
67. A. Rahman and S. B. Jonnalagadda, *Catal. Lett*., 2008, **123**, 264.
68. S. Gu, S. Wunder, Y. Lu and M. Ballauff. *J. Phys. Chem. C*, 2014, **118**, 18618.
69. S. Farhadi, M. Kazem and F. Siadatnasab, *Polyhedron,* 2011, **30**, 606.
70. D. M. Newns, *Phys. Rev.,* 1969, **178**, 1123.
71. B. Hammer, J. K. Norskov, *Nature*, 1995, **376**, 238.
72. P. Lu, T. Teranishi, K. Asakura, M. Miyake, N. J. Toshima, *Phys. Chem. B*, 1999, **103**, 9673.
73. A. Logadottir, T. H. Rod, J. K. Norskov, B. Hammer, S. Dahl, C. J. H. Jacobsen, *J. Catal*., 2001, **197**, 229.
74. L. K. Yeung, R. M. Crooks, *Nano Lett*., 2001, **1**, 14−17.
75. R. W. J. Scott, O. M. Wilson, S.-K. Oh, E. A. Kenik, R. M. Crooks*, J. Am. Chem. Soc*. 2004, **126**, 15583.
76. O. M. Wilson, R. W. J. Scott, J. C. Garcia-Martinez, R.M. Crooks, *J. Am. Chem. Soc*., 2005, **127**, 1015.
77. Z. D. Pozun, S. E. Rodenbusch, E. Keller, K. Tran, W. Tang, K. J. Stevenson and G. Henkelman, *J. Phys. Chem. C*, 2013, **117**, 7598.
78. I. Langmuir, *Trans. Faraday Soc*., 1922, **17**, 621.
79. C. N. Hinshelwood, *Ann. Res. London Chem. Soc.,* 1930, **27**, 11.
80. P. W. Atkins, Physical Chemistry (Oxford Univ. Press, London, 1985), 3rd ed., 782.
81. J. Harris and B. Kasemo, *Surf. Sci*., 1981, **105**, 281.
82. K. Sinniah, M. G. Sherman, L. B. Lewis, W. H. Weinberg, J. T. Yates, and K. C. Janda, *Phys. Rev. Lett.*, 1989, **62**, 567.
83. W. Stefanie, P. Frank, L. Yan, M. Yu and M. Ballauf, *J. Phys. Chem. C,* 2010, **114***,* 8814.
84. Y. Khalavka, J. Becker and C. Sonnichsen. *J. Am. Chem. Soc.,* 2009, **131**, 1871.
85. D. Eley and E. K. Rideal, *Nature (London),* 1940, **146**, 401.
86. D. Eley, *Proc. Roy. Soc. London,* 1941, **178**, 452.
87. A. Panacek, R. Prucek, J. Hrbac, T. Nevecna, J. Steffkova, R. Zboril and L. Kvitek, *Chem. Mater.,* 2014, **26**, 1332.
88. A. Danon and A. Amirav, *J. Phys. Chem.,* 1989, **93**, 5549.
89. A. Danon and A. Amirav, *Isr. J. Chem.,* 1989, **29**, 443.
90. A. Danon, A. Vardi, and A. Amirav, *Phys. Rev. Lett.,* 1990, **65**, 2038.
91. A. Danon and A. Amirav, *Phys. Rev. Lett.,* 1988, **61**, 2961.
92. A. Danon and A. Amirav, *J. Chem. Phys.*, 1987, **86**, 4708.
93. A. Danon, E. Kolodney and A. Amirav, *Surf. Sci.,* 1988, **193**, 132.
94. A. Danon and A. Amirav, *J. Chem. Phys.*, 1990, **92**, 6968.
95. A. Danon and A. Amirav, *Int. J. Mass. Spectrom. Ion Processes,* 1990, **96**, 139.
96. C. T. Campbell, G. Ertl, H. Kuipers, and J. Segner, *J. Chem. Phys.,* 1980, **73**, 5862.
97. E. Y. Zandberg and U. K. Rasulev, *Russ. Chem. Rev.,* 1982, **51**, 819.
98. M. E. M. Spruit and A. W. Kleyn, *Chem. Phys. Lett.*, 1989, **159**, 342.
99. E. W. Kuipers, A. Vardi, A. Danon and A. Amirav, *Phys. Rev. Lett.,* 1991, **66**, 116-119.
100. J. D. Beckerle, Q. Y. Yang, A. D. Johnson and S. T. Ceyer, *J. Chem. Phys.,* 1987, **86**, 7236.
101. S. Sarkar, A. K. Guria and N. Pradhan. *Chem. Commun.*, 2013, **49**, 6018.
102. F. Mahdavi, T. C. Bruton and Y. Li, *J. Org. Chem.,* 1993,**58**, 744.
103. Y. Su, J. Lang, L. Li, K. Guan, C. Du, L. Peng, D. Han and X. Wang, *J. Am. Chem. Soc.*, 2013, **135**, 11433.

104. E. A. Reyes-Garcia, Y. P. Sun, K. Reyes-Gil and D. Raftery, *J. Phys. Chem. C*, 2007, **111**, 2738.
105. Q. P. Wu and R. van de Krol, *J. Am. Chem. Soc*. 2012, **134**, 9369.
106. R. Schaub, E. Wahlstron, A. Ronnau, E. Laegsgaard, I. Stensgaard and F. Besenbacher, *Science,* 2003, **299**, 377.
107. W.–Y. Ahn, S. A. Sheeley, T. Rajh and D. M. Cropek, *Appl. Catal. B: Environ*, 2007, **74**, 103.
108. V. Brezova, A. Blazkova, I. Surina and B. Havlinova, *J. Photochem. Photobiol. C,* 1997, **107,** 233.
109. H. Kominami, K. Nakanishi, S. Yaamamoto, K. Imamura and K. Hashimoto, *Catal. Commun.*, 2014, **54**, 100.
110. A. Hakki, R. Dillert and D. W. Bahnemann, *Phys. Chem. Chem. Phys*., 2013, **15**, 2992.
111. M. Hecht, W. R. Fawcett, *J. Phys. Chem.,* 1995, **99**, 1311.
112. P. J. Reid, P. F. Barbara, *J. Phys. Chem*., 1995, **99**, 3554.
113. M. Opallo, *J. Chem. Soc., Faraday Trans*., 1986, **182**, 339.
114. R. Chen, G. R. Freeman, *J. Phys. Chem*., 1995, **99**, 4970.
115. M. J. Kamlet, J.–L. M. Abboud, M. H. Abraham, R. W. Taft, *J. Org Chem*., 1983, **48**, 2877.
116. Y. Marcus, Chem. *Soc. Rev.*, 1993, **22**, 409.
117. J. Zeng, Q. Zhang, J. Chen and Y. Xia, *Nano Lett.,* 2010, **10**, 30.
118. K. S. Chin, J.-Y. Choi, C. S. Park, H. J. Jang and K. Kim, *Catal. Lett.,* 2009, **133**, 1.
119. S. Saha, A. Pal, S. Kundu, S. Basu and T. Pal, *Langmuir,* 2010, **26**, 2885.
120. T. K. Sau, A. Pal and T. Pal, *J. Phys. Chem. B*, 2001, **105**, 9266.
121. S. Dutta, S. Sarkar, C. Ray, A. Roy, R. Sahoo and T. Pal, *ACS Appl. Mater. Interfaces,* 2014, **6**, 9134.
122. S. K. Ghosh, M. Mandal, S. Kundu, S. Nath and T. Pal, *Appl. Catal. A: Gen.,* 2004, **268**, 61.
123. S. Sarkar, A. K. Sinha, M. Pradhan, M. Basu, Y. Negishi and T. Pal, *J. Phys. Chem. C*, 2011, **115**, 1659.
124. S. Jana, S. K. Ghosh, S. Nath, S. Pande, S. Praharaj, S. Panigrahi, S. Basu, T. Endo and T. Pal, *Appl. Catal. A: Gen.,* 2006, **313**, 41.
125. K. K. Haldar, S. Kundu, and A. Patra, *ACS Appl. Mater. Interfaces*, 2014, **6**, 21946.
126. R. Ciganda, N. Li, C. Deraedt, S. Gatard, P. Zhao, L. Salmon, R. Hernandez, J. Ruiza and D. Astruc, *Chem. Commun.,* 2014, **50**, 10126.
127. C. Deraedt, L. Salmon, S. Gatard, R. Ciganda, R. Hernandez, J. Ruiza and D. Astruc, *Chem. Commun.,* 2014, **50**, 14194.
128. D. Astruc, *Nat. Chem*., 2012, **4**, 255.
129. R. Nie, J. Wang, L. Wang, Y. Qin, P. Chen and Z. Hou, *Carbon,* 2012, **50**, 586.
130. D. Shah and H. Kaur, *J. Mol. Catal. A: Chem.,* 2014, **381**, 70.
131. R. J. Kalbasi, A. A. Nourbakhsh and F. Babaknezhad, *Catal. Commun.,* 2011, **12**, 955.
132. S. Zhang, S. Gai, F. He, S. Ding, L. Li and P. Yang, *Nanoscale*, 2014, **6**, 11181.
133. N. Lu, W. Chen, G. Fang, B. Chen, K. Yang, Y. Yang, Z. Wang, S. Huang and Y. Li, *Chem. Mater.,* 2014, **26**, 2453.
134. B. Sreedhar, D. K. Devi, D. Yada, *Catal. Commun.,* 2011, **12**, 1009.
135. H.-S. Shin and S. Huh*, ACS Appl. Mater. Interface,* 2012, **4**, 6324.
136. J. Lee, J. C. Park, J. U. Bang and H. Song, *Chem. Mater.,* 2008, **20**, 5839.
137. J. Min, F. Wang, Y. Cai, S. Liang, Z. Zhang and X. Jiang, *Chem. Commun.*, 2015, **51**, 761.
138. P. Luo, K. Xu, R. Zhang, L. Huang, J. Wang, W. Xing and J. Huang, *Catal. Sci. Technol.,* 2012, **2**, 301.
139. L. Li, Z. Niu, S. Cai, Y. Zhi, H. Li, H. Rong, L. Liu, L. Liu, W. He and Y. Li, *Chem. Commun.,* 2013, **49**, 6843.
140. C.–H. Tang, L. He, Y.–M. Liu, Y. Cao, H.–Y. He and K.–N. Fan, *Chem. Eur. J.,* 2011, **17**, 7172.
141. M. Dasog, W. Hou and R. W. J. Scott, *Chem. Commun.,* 2011, **47**, 8569.
142. M. Brust, M. Walker, D. Bethell, D. J. Schiffrin and R. J. Whyman, *J. Chem. Soc., Chem. Commun.*, 1994, 801.
143. A. C. Templeton, W. P. Wuelfing and R. W. Murray, *Acc. Chem. Res*., 2000, **33**, 27.
144. B. Liu, W. Zhang, H. Feng and X. Yang, *Chem. Commun.,* 2011, **47**, 11727.
145. Y. Deng, Y. Cai, Z. Sun, J. Liu, C. Liu, J. Wei, W. Li, C. Liu, Y. Wang and D. Zhao, *J. Am. Chem. Soc***.,** 2010, **132,** 8466.
146. S. Wang, M. Zhang and W. Zhang *ACS Catal.,* 2011, **1**, 207.
147. S. N. Shmakov, Y. Jia, and E. Pinkhassik, *Chem. Mater.* 2014, **26**, 1126.
148. K. Kamata, Y. Lu and Y. Xia, *J. Am. Chem. Soc.*, 2003, **125**, 2384.
149. X. W. Lou, L. A. Archer and Z. C. Yang, *Adv. Mater.*, 2008, **20**, 3987.
150. S. N. Shmakov and E. Pinkhassik, *Chem. Commun*., 2010, **46**, 7346.
151. Y. J. Hong, M. Y. Son, B. K. Park, Y. C. Kang, *Small,* 2013, **9**, 2224.
152. T. Huang, F. Meng and L. M. Qi, *J. Phys. Chem. C*, 2009, **113**, 13636.
153. S. A. Dergunov, K. Kesterson, W. Li, Z. Wang and E. Pinkhassik, *Macromolecules*, 2010, **43**, 7785.
154. S. A. Dergunov and E. Pinkhassik, *Angew. Chem., Int. Ed.* 2008, **47**, 8264.
155. D. C. Danila, L. T. Banner, E. J. Karimova, L. Tsurkan, X. Y. Wang and E. Pinkhassik, *Angew. Chem., Int. Ed.* 2008, **47**, 7036.
156. D. H. W. Hubert, M. Jung and A. L. German, *Adv. Mater.,* 2000, **12**, 1291.
157. J. Hotz and W. Meier, *Langmuir*, 1998, **14**, 1031.
158. W. Meier, *Chem. Soc. Rev*., 2000, **29**, 295.
159. N. Yan, Z. Zhao, Y. Li, F. Wang, H. Zhong, and Q. Chen., *Inorg. Chem.,* 2014, **53**, 9073.
160. B. Liu, Y. Niu, Y. Li, F. Yang, J. Guo, Q. Wang, P. Jing, J. Zhang and G. Yun. *Chem. Commun.,* 2014, **50**, 12356.
161. Y. Li and J. Shi, *Adv. Mater*., 2014, **26**, 3176.
162. J. Liu, S. Z. Qiao, J. S. Chen, X. W. Lou, X. Xing and G. Q. Lu*, Chem. Commun.*, 2011, **47**, 12578.

163. J. Liu, H. Q. Yang, F. Kleitz, Z. G. Chen, T. Yang, E. Strounina, G. Q. Lu and S. Z. Qiao, *Adv. Funct. Mater.*, 2012, **22**, 591.
164. Z. Chen, Z.-M. Cui, P. Li, C.-Y. Cao, Y.-L. Hong, Z.-Y. Wu and W.-G. Song, *J. Phys. Chem. C*, 2012, **116**, 14986.
165. J. Wei, H. Wang, Y. Deng, Z. Sun, L. Shi, B. Tu, M. Luqman and D. Zhao, *J. Am. Chem. Soc.,* 2011, **133**, 20369.
166. H. Lang, S. Maldonado, K. J. Stevenson and B. D. Chandler, *J. Am. Chem. Soc*., 2004, **126**, 12949.
167. G. Vijayaraghavan and K. J. Stevenson, *Langmuir*, 2007, **23**, 5279.
168. N. M. Bedford, R. Bhandari, J. M. Slocik, S. Seifert, R. R. Naik and M. R. Knecht, *Chem. Mater.,* 2014, **26**, 4082.
169. K. A. Marvin, N. N. Thadani, C. A. Atkinson, E. L. Kellerc and K. J. Stevenson, *Chem. Commun*., 2012, **48**, 6289.
170. N. Li, M. Echeverria, S. Moya, J. Ruiz and D. Astruc, *Inorg., Chem*., 2014, **53**, 6954.
171. J. C. Garcia-Martinez, R. Lezutekong and R. M. Crooks. *J. Am. Chem. Soc.*, 2005, **127**, 5097.
172. R. W. J. Scott, C. Sivadinarayana, O. M. Wilson, Z. Yan, D. W. Goodman and R. M. Crooks, *J. Am. Chem. Soc.,* 2005, **127**, 1380.
173. E. Seo, J. Kim, Y. Hong, Y. S. Kim, D. Lee and B.-S. Kim, *J. Phys. Chem. C,* 2013, **117**, 11686.
174. R. J. Rahaim, Jr. and R. E. Maleczka, Jr., *Org. Lett.*, 2005, **7**, 5087.
175. M. Takasaki, Y. Motoyama, K. Higashi, S.-H. Yoon, I. Mochida and H. Nagashima, *Org. Lett.*, 2008, **10**, 1601.
176. J. Dhar and S. Patil, *ACS Appl. Mater. Interfaces,* 2012, **4**, 1803.
177. M. Liang, R. Su, R. Huang, W. Qi, Y. Yu, L. Wang and Z. He, *ACS Appl. Mater. Interfaces*, 2014, **6**, 4638.
178. H. Wang, H. Ma, W. Zheng, D. An and C. Na, *ACS Appl. Mater. Interfaces,* 2014, **6**, 9426.
179. H. Zhang, L. Ye, X. Wang, F. Li and J. Wang, *Chem. Commun.,* 2014, **50**, 2565.
180. J.-H. Kim, K. M. Twaddle, J. Hu and H. Byun, *ACS Appl. Mater. Interfaces,* 2014, **6**, 11514.
181. H. Yang, K. Nagai, T. Abe, H. Homma, T. Norimatsu and R. Ramaraj, *ACS Appl. Mater. Interfaces,* 2009, **1**, 1860.
182. L. M. Liz-Marzan, M. Giersig and P. Mulvaney, *Langmuir*, 1996, **12**, 4329.
183. Z. W. Seh, S. Liu, S.-Y. Zhang, K. W. Shaha and M.-Y. Han, *Chem. Commun*., 2011, **47**, 6689.
184. C.-H. Liu, X.-Q. Chen, Y.-F. Hu, T.-K. Sham, Q. J. Sun, J.-B. Chang, X. Gao, X.-H. Sun and S.-D. Wang, *ACS Appl. Mater. Interfaces*, 2013, **5**, 5072.
185. R. Li, P. Zhang, Y. Huang, C. Chen and Q. Chen, *ACS Appl. Mater. Interfaces*, 2013, **5**, 12695.
186. A. S. Peinetti, S. Herrera, G. A. Gonzalez and F. Battaglini. *Chem. Commun.,* 2013, **49**, 11317.
187. R.-Y. Zhong, K.-Q. Sun, Y.-C. Hong and B.-Q. Xu, *ACS Catal.*, 2014, **4**, 3982.
188. N. Yan, J. Zhang, Y. Yuan, G.-T. Chen, P. J. Dyson, Z.-C. Li and Y. Kou , *Chem. Commun.*, 2010, **46**, 1631.
189. H. You, Z. Peng, J. Wua and H. Yang, *Chem. Commun*., 2011, **47**, 12595.
190. R. He, Y.-C. Wang, X. Wang, Z. Wang, G. Liu, W. Zhou, L. Wen, Q. Li, X. Wang, X. Chen, J. Zeng and J. G. Hou, *Nat. Commun.*, DOI: 10.1038/ncomms5327.
191. G. He, W. Liu, X. Sun, Q. Chen, X. Wang, H. Chen, *Mater. Res. Bull*., 2013, **48**, 1885.
192. W. S. Hummers and R. E. Offeman, *J. Am. Chem. Soc.,* 1958, **80**, 1339.
193. N. I. Kovtyukhova, P. J. Ollivier, B. R. Martin, T. E. Mallouk, S. A. Chizhik, E. V. Buzaneva and A. D. Gorchinskiy, *Chem. Mater.,* 1999, **11**, 771.
194. J. W. Larsen, M. Freund, K. Y. Kim, M. Sidovar and J. L. Stuart, *Carbon* 2000, **38**, 655.
195. P. S. Kumbhar, J. Sanchez-Valente, J. M. M. Millet, F. Figueras, *J. Catal.,* 2000, **191**, 467.
196. K. Selvam and M. Swaminathan, *J. Mol. Catal. A: Chem.,* 2011, **351**, 52.
197. N. Sobana, M. Muruganandham, M. Swaminathan, *J. Mol. Catal.,* 2006, **258,** 124.
198. J. Davarpanah and A. R. Kiasat, *Catal. Commun.,* 2013, **41**, 6.
199. D. Cantillo, M. Baghbanzadeh and C. O. Kappe, *Angew. Chem.Int. Ed*., 2012, **51**, 10190.
200. D. Cantillo, M. M. Moghaddam, C. O. Kappe *J. Org. Chem*., 2013, **78**, 4530.
201. W.-W. Wang, Y.-J. Zhu, M.-L.Ruan, *J. Nanopart. Res.,* 2007, **9**, 419.
202. E. A. Osborne, T. M. Atkins, D. A. Gilbert, S. M. Kauzlarich, K. Liu and A. Y. Louie, *Nanotechnology,* 2012, **23**, 215602.
203. N. Perret, F. Cardenas-Lizana, D. Lamey, V. Laporte, L. Kiwi-Minsker and M. A. Keane, *Top Catal.,* 2012, **55**, 955.
204. D. Stibal, J. Sa and J. A. van Bokhoven, *Catal. Sci. Technol.,* 2013, **3**, 94.
205. G.-H. Wang, Q. Sun, R. Zhang, W.-C. Li, X.-Q. Zhang and A.-H. Lu, *Chem. Mater.,* 2011, **23**, 4537.
206. J. Y. Kim, S. B. Yoon, J.-S. Yu, *Chem. Commun.,* 2003, 790.
207. S. Ikeda, S. Ishino, T. Harada, N. Okamoto, T. Sakata, H. Mori, S. Kuwabata, T. Torimoto and M. Matsumura, *Angew. Chem., Int. Ed*., 2006, **45**, 7063.
208. T. Valdes-Solis, P. Valle-Vigon, M. Sevilla and A. B. Fuertes, *J. Catal.,* 2007, **251**, 239.
209. A. B. Fuertes, M. Sevilla, T. Valdes-Solis and P. Tartaj, *Chem. Mater.,* 2007, **19**, 5418.
210. M. Shokouhimehr, J. E. Lee, S. I. Hana and T. Hyeon, *Chem. Commun.,* 2013, **49**, 4779.
211. R. Raja, V. B. Golovko, J. M. Thomas, A. Berenguer-Murcia, W. Zhou, S. Xiee and B. F. G. Johnsona, *Chem. Commun*., 2005, **15**, 2026.
212. R. Dey, N. Mukherjee, S. Ahammed and B. C. Ranu, *Chem. Commun.,* 2012, **48**, 7982.
213. X. Gu, Z. Sun, S. Wu, W. Qi, H. Wang, X. Xu and D. Su. *Chem. Commun.,* 2013, **49**, 10088.
214. M. Paul, N. Pal and A. Bhaumik. *Eur. J. Inorg. Chem.,* 2010, 5129.
215. M. B. Gawande, A. K. Rathi, P. S. Branco, I. D. Nogueira, A. Velhinho, J. J. Shrikhande, U. U. Indulkar, R. V. Jayaram, C.

A. A. Ghumman, N. Bundaleski and O. M. N. D. Teodoro . *Chem. Eur. J.,* 2012, **18**, 12628.
216. D. Cantillo, M. M. Moghaddam and C. O. Kappe, *J. Org. Chem.,* 2013, **78**, 4530.
217. H. K. Kadam and S. G. Tilve, *RSC Adv.*, 2012, **2**, 6057.
218. J. Pal, C. Mondal, A. Kumar Sasmal, M. Ganguly, Y. Negishi and T. Pal, *ACS Appl. Mater. Interfaces,* 2014, **6**, 9173.
219. R. Liu, Y. Guo, G. Odusote, F. Qu and R. D. Priestley, *ACS Appl. Mater. Interfaces*, 2013, **5**, 9167.
220. B. Liu, S. Yu, Q. Wang, W. Hu, P. Jing, Y. Liu, W. Jia, Y. Liu, L. Liua and J. Zhang, *Chem. Commun.,* 2013, **49**, 3757.
221. S. Stankovich, D. A. Dikin, G. H. Dommett, K. M. Kohlhaas, E. J. Zimney, E. A. Stach, R. D. Piner, S. T. Nguyen, R. S. Ruoff, *Nature*, 2006, **442**, 282.
222. N. Li, Y. Xiao, C. Hu and M. Cao, *Chem., Asian J.,* 2013, **8**, 1960.
223. P. Wang, J. Wang, T. Ming, X. Wang, H. Yu, J. Yu, Y. Wang and M. Lei, *ACS Appl. Mater. Interfaces*, 2013, **5**, 2924.
224. Y. Lin and J. W. Connell, *Nanoscale*, 2012, **4**, 6908.
225. S. Praharaj, S. Nath, S. K. Ghosh, S. Kundu, and T. Pal. *Langmuir,* 2004, **20***,* 9889.
226. Y. Choi, H. S. Bae, E. Seo, S. Jang, K. H. Park and B.–S. Kim, *J. Mater. Chem.*, 2011, **21**, 15431.
227. E. K. Jeon, E. Seo, E. Lee, W. Lee, M.–K. Um and B.–S. Kim. *Chem. Commun.,* 2013, **49**, 3392.
228. S. Bai, X. Shen, G. Zhu, M. Li, H. Xi and K. Chen, *ACS Appl. Mater. Interfaces,* 2012, **4**, 2378.
229. C. Huang, W. Ye, Q. Liu and X. Qiu, *ACS Appl. Mater. Interfaces,* 2014, **6**, 14469.
230. W. Lei, D. Portehault, D. Liu, S. Qin and Y. Chen, *Nat. Commun.*, 2013, **4**, 1777.
231. W. Chen, Y. Li, G. Yu, C.–Z. Li, S. B. Zhang, Z. Zhou and Z. Chen, *J. Am. Chem. Soc*., 2010, **132**, 1699.
232. R. Haubner, M. Wilhelm, R. Weissenbacher and B. Lux. Jansen, M., Ed., Springer: Berlin Heidelberg, 2002.
233. K. Watanabe, T. Taniguchi and H. Kanda, *Nat. Mater.,* 2004, **3**, 404.
234. K. Watanabe, T. Taniguchi, T. Niiyama, K. Miya, M. Taniguchi, *Nat. Photonics,* 2009, **3**, 591.
235. W. Lei, D. Portehault, R. Dimova and M. Antonietti, *J. Am. Chem. Soc.,* 2011, **133**, 7121.
236. L. H. Li, Y. Chen, B.-M. Cheng, M. Y. Lin, S. L. Chou and Y. C. Peng, *Appl. Phys. Lett.,* 2012, **100**, 261108.
237. Y. Lin and J. W. Connell, *Nanoscale*, 2012, **4**, 6908.
238. Y. Lin, T. V. Williams, T. B. Xu, W. Cao, H. E. Elsayed-Ali, J. W. Connell, *J. Phys. Chem. C,* 2011, **115**, 2679.
239. C.-C. Yeh, P.-R. Wu, D.-H. Chen, *Mater. Lett.*, 2014, **136**, 274.
240. X. Le, Z. Dong, W. Zhang, X. Li and J. Ma, *J. Mol. Catal. A: Chem.,* 2014, 395, 58.
241. B. Adhikari, A. Biswas, and A. Banerjee. *ACS Appl. Mater. Interfaces,* 2012, **4**, 5472.
242. A. Zinchenko, Y. Miwa, L. I. Lopatina, V. G. Sergeyev and S. Murata*, ACS Appl. Mater. Interfaces,* 2014, **6**, 3226.
243. A. A. Zinchenko, Polym. *Sci., Ser. C*, 2012, **54**, 80.
244. C. Mandal and U. S. Nandi, *Proc. Ind. Acad. Sci.* 1979, **88**, 263.
245. S. Y. Pu, A. A. Zinchenko and S. Murata, *Langmuir*, 2011, **27**, 5009.
246. S. Y. Pu, A. A. Zinchenko and S. Murata, *J. Nanosci. Nanotechnol.* 2012, **12**, 635.
247. Y. L. Geng, J. F. Liu, E. Pound, S. Gyawali, J. N. Harb and A. T. Woolley, *J. Mater. Chem.* 2011, **21**, 12126.
248. C. K. S. Pillai and U. S. Nandi, *Biopolymers,* 1973, **12,** 1431.
249. J. F. Liu, Y. L. Geng, E. Pound, S. Gyawali, J. R. Ashton, J. Hickey, A. T. Woolley and J. N. Harb, *ACS Nano*, 2011, **5**, 2240.
250. Y. W. Kwon, C. H. Lee, D. H. Choi and J. I. Jin, *J. Mater. Chem.*, 2009, **19**, 1353.
251. J. Chen, P. Xiao, J. Gu, D. Han, J. Zhang, A. Sun, W. Wang and T. Chen. *Chem. Commun.,* 2014, **50**, 1212.
252. J. Zhang, D. Han, H. Zhang, M. Chaker, Yue Zhao and D. Ma, *Chem. Commun.,* 2012, **48**, 11510.
253. S. Fountoulaki, V. Daikopoulou, P. L Gkizis, I. Tamiolakis, G. S. Armatas and I. N. Lykakis, *ACS Catal*., 2014, **4**, 3504.
254. P. Veerakumar, R. Madhu, S.-M. Chen, V. Veeramani, C.-T. Hung, P.-H. Tang, C.-B. Wang and S.-B. Liu, *J. Mater. Chem. A*, 2014, **2**, 16015.
255. P. Pachfule, S. Kandambeth, D. D. Diaz and R. Banerjee, *Chem. Commun.,* 2014, **50**, 3169.
256. S. Kandambeth, A. Mallick, B. Lukose, M. V. Mane, T. Heine and R. Banerjee, *J. Am. Chem. Soc*., 2012, **134**, 19524.
257. H.–L. Jiang, T. Akita, T. Ishida, M. Haruta and Q. Xu, *J. Am. Chem. Soc*., 2011, **133**, 1304.
258. Z. Li and H. C. Zeng, *J. Am. Chem. Soc*., 2014, **136**, 5631.
259. M. Mullner, T. Lunkenbein, J. Breu, F. Caruso and A. H. E. Muller, *Chem. Mater*., 2012, **24**, 1802.
260. X. Wang, D. Liu, S. Song and H. Zhang, *J. Am. Chem. Soc*. 2013, **135**, 15864.
261. T. Wen, D.–X. Zhang, H.–X. Zhang, H.–B. Zhang, J. Zhang and D.–S. Li, *Chem. Commun.,* 2014, **50**, 8754.
262. T. H. Noh, J. Jang, W. Hong, H. Lee and O.-S. Jung, *Chem. Commun.,* 2014, **50**, 7451.
263. P. Deka, R. C. Deka and P. Bharali, *New J. Chem.,* 2014, **38**, 1789.
264. A. Dalui, U. Thupakula, A. H. Khan, T. Ghosh, B. Satpati and S. Acharya, *Small*, 2014, DOI: 10.1002/smll.201402837
265. J. Nanda, A. Biswas, B. Adhikari and A. Banerjee, *Angew. Chem. Int. Ed*., 2013, **52**, 5041.